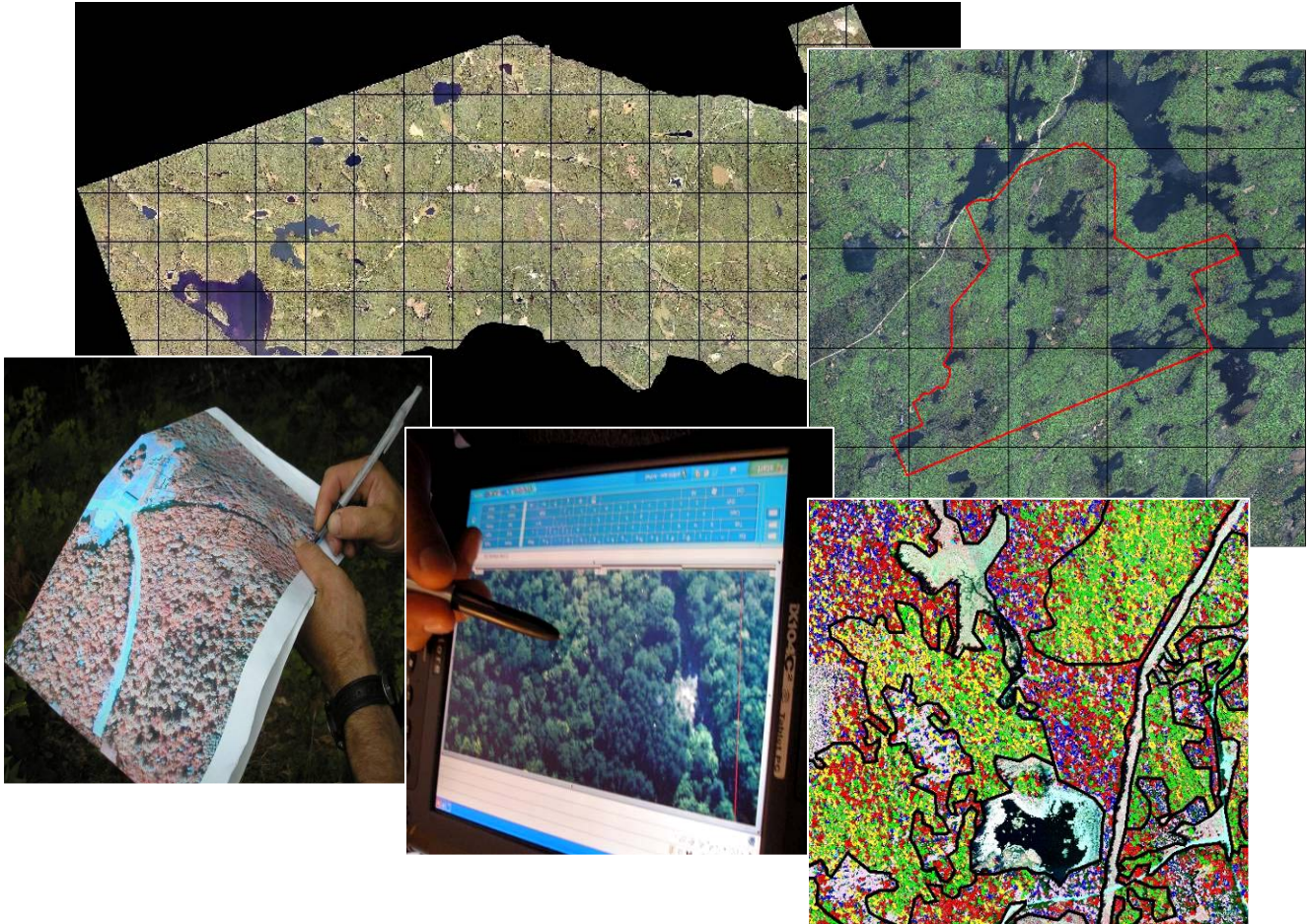


Semi-Automated Species Classification in Ontario Great Lakes–St. Lawrence Forest Conditions

M. Chubey¹, K. Stehle¹, R. Albricht¹, F. Gougeon², D. Leckie², S. Gray², M. Woods³, and P. Courville⁴

January 2009



FORESTRY FUTURES TRUST ONTARIO



Natural Resources
Canada

Ressources naturelles
Canada

Canadian Forest
Service

Service canadien
des forêts



¹ Silvatech Consulting Ltd., P.O. Box 1030, Salmon Arm, BC, V1E 4P2

² Pacific Forestry Centre, 506 West Burnside Rd., Victoria, BC, V8Z 1M5

³ Ontario Ministry of Natural Resources, 3301 Trout Lake Rd., North Bay, ON, P1A 4L7

⁴ Forestry Research Partnership, P.O. Box 430, 6905 Hwy 17 W., Mattawa, ON, P0H 1V0

Acknowledgments:

This project could not have happened without the enthusiasm of Murray Woods and the support of the Forest Research Partnership (John Pineau, Ken Durst, and Paul Courville) and Dave Nesbitt of the Ontario Ministry of Natural Resources (OMNR). Equally important has been the contribution of the Canadian Forest Service (CFS) Digital Remote Sensing project. The staff and caretakers of the Petawawa Research Forest of the Canadian Forest Service and Swan Lake Research Forest of the OMNR are also acknowledged for their support.

Financial support is greatly acknowledged from the Forestry Futures Trust—Enhanced Forest Productivity Fund along with the Forest Research Partnership and the extensive in-kind support of the OMNR and the CFS.

Table of Contents

| | | |
|----------|--|----|
| 1. | Introduction..... | 1 |
| 2. | Objectives | 1 |
| 3. | Background..... | 2 |
| 3.1. | Enhanced Forest Resource Inventory Paradigm..... | 2 |
| 3.2. | Individual Tree Crown (ITC) Approach..... | 2 |
| 3.3. | Research Partners..... | 3 |
| 4. | Study Area and Data..... | 3 |
| 4.1. | Location and description of study sites..... | 3 |
| 4.2. | Description of imagery and LiDAR data..... | 5 |
| 4.3. | Description of field data..... | 6 |
| 5. | Methods..... | 6 |
| 5.1. | Field data collection and classifier training methods..... | 7 |
| 5.1.1. | <i>Method 1</i> | 8 |
| 5.1.2. | <i>Method 2</i> | 9 |
| 5.1.3. | <i>Method 3</i> | 9 |
| 5.1.4. | <i>Method 4</i> | 10 |
| 5.1.5. | <i>Method 5</i> | 11 |
| 5.2. | Data analysis methods..... | 12 |
| 5.2.1. | <i>Introduction</i> | 12 |
| 5.2.2. | <i>Operational Considerations</i> | 15 |
| 5.2.3. | <i>Preliminary Image Processing</i> | 15 |
| 5.2.3.1. | <i>LiDAR-Based Masking</i> | 15 |
| 5.2.3.2. | <i>BRDF Correction – Image Normalization</i> | 16 |
| 5.2.4. | <i>ITC Suite Processing</i> | 17 |
| 5.2.5. | <i>Post-Processing</i> | 19 |
| 5.2.6. | <i>Production Times</i> | 19 |
| 5.2.6.1. | <i>Field Data Collection and Classifier Training Time Requirements</i> | 19 |
| 5.2.6.2. | <i>Image Preparation and Processing</i> | 20 |
| 5.2.6.3. | <i>Manual Editing of Stand Delineation</i> | 21 |
| 5.2.6.4. | <i>GIS Operations to Populate Database</i> | 21 |
| 6. | Preliminary Results and Discussion..... | 22 |
| 6.1. | Introduction..... | 22 |
| 6.2. | Tree Crown Delineation..... | 22 |
| 6.3. | Species Classification | 24 |
| 6.3.1. | <i>Swan Lake Species Signatures and Classification with Methods 1 - 3</i> | 24 |
| 6.3.2. | <i>Petawawa Research Forest Species Signatures and Classification with Methods 1-3</i> | 27 |
| 6.3.3. | <i>Petawawa Research Forest Classification with Method 4</i> | 27 |
| 6.3.4. | <i>Petawawa Research Forest Classification with Method 5</i> | 31 |
| 6.4. | Forest Stand Polygon Delineation | 34 |
| 6.5. | The Role of LiDAR | 38 |
| 7. | Challenges and Associated Consequences..... | 41 |
| 7.1. | Imagery Issues | 41 |
| 7.2. | Date of Image Acquisition (Leaf Status) | 41 |
| 7.3. | Implementation Hurdles..... | 41 |
| 8. | Summary of Achievements..... | 43 |

| | |
|---|----|
| 9. Opportunities for Future R&D and Testing Efforts | 44 |
| Bibliography | 46 |
| Appendix 1 | 48 |

List of Figures

| | |
|--|----|
| Figure 1. Map of study sites in Ontario. | 4 |
| Figure 2. Species training methods..... | 7 |
| Figure 3. Recording the centre of a tree crown in Swan Lake with the Trimble ProXT and Hurricane antenna on a ‘ruggedized’ laptop..... | 8 |
| Figure 4. Creating tree crown polygon from GPS positional information. | 8 |
| Figure 5. Identifying and marking points on clusters of tree crowns on the data tablet in the field as used in Method 3. | 9 |
| Figure 6. Examples of sizeable single species areas delineated on the screen in the fourth method of signature acquisition. | 11 |
| Figure 7. Plots of individual tree crowns of large toothed aspen (Alt) from three training sets making obvious the outliers to be removed in order to purify the signature. | 11 |
| Figure 8. Plots of individual tree crowns of larch from four (4) training sets making obvious why larch crowns were broken into two classes, later named normal larch (La nm) and bright larch (La br)..... | 12 |
| Figure 9. Plot of signatures in multispectral space (near infrared vs. red) illustrating the potential separability of classes (or lack thereof) from this particular point of view. | 13 |
| Figure 10. Plot of signatures in multispectral space (green vs. blue) illustrating the potential separability of classes (or lack thereof) from this particular point of view. | 13 |
| Figure 11. Sub-area (7 km x 8 km) of the Petawawa Research Forest supplied ortho-mosaic as used with Method 5. Even after substantial Bidirectional Reflectance Distribution Function (BRDF) and normalization efforts, the image still exhibits how some parts of the area appear relatively well-balanced radiometrically while other parts (low centre) appear normalized different. | 14 |
| Figure 12. Preliminary processing workflow..... | 16 |
| Figure 13. ITC approach workflow: individual tree crown delineation and ITC approach workflow: individual tree crown delineation and classification (based on Gougeon, 1997). | 17 |
| Figure 14. ITC approach workflow: forest stand polygon delineation (based on Gougeon, 1997). | 18 |
| Figure 15. Theorized manual and automated productivity comparison. | 21 |

| | |
|---|----|
| Figure 16. ITC delineation example (Swan Lake); scale = 1:1,000. | 23 |
| Figure 17. Classification and delineation result: Swan Lake (67504_A4). | 25 |
| Figure 18. Classification and delineation result: Swan Lake (67503_D4). | 26 |
| Figure 19. Classification and delineation result: Petawawa validation area. | 28 |
| Figure 20. Delineation result: Swan Lake (67504_A4). | 35 |
| Figure 21. Delineation result: Swan Lake (67503_D4). | 36 |
| Figure 22. Delineation result: Petawawa validation area. | 37 |
| Figure 23. Comparison of spectral-based masking (b) versus LiDAR-based masking (c). | 39 |
| Figure 24. Non-forest areas such as clearings and forest gaps (a) are excluded from analysis using a LiDAR-based mask (b); subsequent ITC analysis is constrained to valid forest areas (c). | 40 |
| Figure A1–1. Colourful rendition of a texture analysis of a M7VI image tile where three distinct mosaicked image strips are visible. Here, the problem is compounded by the fact that each image strip is also acquired with three distinct lenses (blurrier vertical lines pointed to by red arrows). | 54 |
| Figure A1–2. Colourful rendition of a texture analysis of a M7VI image tile showing the ripples caused by the vertical aspect of the radial distortion, as image segments made of 100–300 lines are arbitrarily picked up in the vertical direction to create the image. | 55 |
| Figure A1–3. Seams line automatically generated by PCI™ Orthoengine used to create the Vexcel orthophoto mosaic. Tiles (individual files) of the mosaic are shown in blue, while segment of original Vexcel images are shown in yellow, with one highlighted in white. The images were acquired during West to East flights. | 56 |
| Figure A1–4. Example of the different image sections that can be found within a 1 km ² tile of the Orthophoto of Vexcel images. A serious overkill considering the original images covered at least 2 x 3 km ² . Just picking up the centre 1 km ² would have been a far superior approach. Also visible on the bottom-left are the effects of cloud removal by manual editing. | 57 |
| Figure A1–5. The blurriness of the bottom part of the image can not be explained by just an attempt to blur the image around the mosaic seams. | 58 |
| Figure A1–6. How the Vexcel panchromatic images are acquired. | 59 |

Figure A1–7. The bottom centre portion of this image appears covered with haze, but this is actually due to improper adjustment between the 9 different panchromatic sections of the image.59

Figure A1–8. Two test areas, one of softwoods and one of hardwoods, were created in the overlapping region of two flight lines from a Leica ADS-40v2 sensor to test the correction capabilities of various BRDF curves.60

Figure A1–9. Curves (for the near infrared band) of radiance tendencies due to the joint effects of the solar illumination angle and the view angle gathered under increasingly specific feature mask.61

List of Tables

| | |
|--|----|
| Table 1. Tree species sampled at the Swan Lake Research Forest..... | 6 |
| Table 2. Tree species sampled at the Petawawa Research Forest..... | 7 |
| Table 3. Time requirement for training site data collection..... | 20 |
| Table 4. Summary of Swan Lake species signature (Jeffries Matisuta Distance) separability analysis..... | 24 |
| Table 5. Summary of species signature (Jeffries Matisuta Distance) separability analysis (Petawawa Research Forest)..... | 27 |
| Table 6. Method 4 confusion matrix (testing areas=training areas) of twelve classes portraying ten species. | 30 |
| Table 7. The confusion matrix of the 16 classes (testing areas=training areas) from the 'purified' signatures obtained with Method 5..... | 32 |
| Table 8. The confusion matrix (testing areas=training areas) for a 14 class classification with Method 5 (dropping two classes)..... | 33 |
| Table 9. The confusion matrix (in %) for the 14 classes in Method 5 when regrouped into the 10 species they represent..... | 34 |
| Table A1-1. Types of airborne and satellite sensors. | 50 |
| Table A1-2. Typical image needs for soft copy interpretation and for computer image analysis. | 51 |
| Table A1-3. Differences in radiances between tree crowns from two test areas (softwoods, hardwoods) from the overlapping zone of two flight lines after different types of feature-based corrections for view and illumination angles (BRDF corrections). | 62 |

1. Introduction

Forest Resource Inventories in Ontario (and North America) have been completed based mainly on manual photo-interpretation for the last several decades. While improvements have been made to the overall method and framework, as reflected by the current Forest Information Manual (FIM) standards, the underlying data acquisition technology and analysis approach is largely the same as that developed during World War II.

Recent developments in digital mapping technologies (e.g. Light Detection and Ranging [LiDAR] and multispectral image sensors) present opportunities to better meet the complex information needs of today's forest resource managers through compilation of integrated resource inventories with rich information content far beyond what is currently available. Extraction of such information requires newly developed analysis tools which remove much of the potential subjective bias associated with manual photo-interpretation. Resulting 'enhanced' forest resource inventories should be more objective, consistent, reliable, and quicker to produce than those currently being constructed through traditional means (e.g. 40% time savings in the stand delineation phase [Castilla, 2006]).

The Individual Tree Crown (ITC) Approach to forest inventory production, developed by the Canadian Forest Service (CFS) over the last 15 years (led by François Gougeon), is an example of a semi-automated method and software package which can transform high resolution digital data into a host of objective tree level based forest resource information products suitable for modern forest management requirements.

2. Objectives

The purpose of this project was to support a broader initiative working on the development of an enhanced forest inventory for two sites in the Great Lakes–St. Lawrence Forest based on digital imagery and LiDAR data.

More specifically, the project tested the operational viability of the ITC approach and attempted to quantify time requirements associated with application of the ITC Software Suite in a production environment. The main focus of the project was on semi-automated production of ITC-based attributes (e.g. species identification, crown closure, density, etc.) for use as input parameters for the estimation of additional enhanced forest inventory metrics (basal area, volume, etc). The improvement of equations relating these base input parameters to final derived attributes (e.g. basal area, volume, etc.) was outside of the scope of this particular project. The operational focus and integration of LiDAR data with high resolution digital imagery builds on previous work from similar ITC analysis studies carried out in the past (e.g. Leckie et al, 2003).

Issues requiring further investigation were identified throughout the course of the project and are summarized in Section 8.

3. Background

3.1. Enhanced Forest Resource Inventory Paradigm

A conventional forest inventory is a subjective one-time interpretation of a picture with a variable bias. Once the photo has been interpreted, the attribute information is fixed and can only be changed through a re-interpretation. Subsequent adjustments based on additional ground sampling will increase the accuracy but will never be able to completely remove the subjective variability of the bias in a cost effective manner; only mitigate it. Subjective inconsistencies in delineation and attributing cannot be removed by means of a sample based approach unless the forest can be stratified in such a way that bias can be isolated from error. Unfortunately, while difficult to do in the first place, this approach will also likely not be a cost effective alternative compared to removing the source of the inconsistencies and replacing it with alternative delineation and attributing techniques that are more precise and objective.

An enhanced forest inventory includes an objective, semi-automated data analysis component as well as manual validation of the automated outputs by certified interpreters to reduce subjective error and increase the information content of the inventory. The entire data set can be reprocessed and/or calibrated if new data or analysis methods are introduced, or requirements change, at a fraction of the cost of a re-interpretation through manual methods. The associated data set is more flexible and can also be 'mined' now, and in the future, to answer additional new resource information questions. The need for subsequent adjustments may be greatly reduced if not removed altogether.

The enhanced forest inventory paradigm presented is built upon the identification of individual tree crowns and 'advances the yardstick' as compared to conventional forest resource inventories, to enable the production of spatially detailed, precise, accurate, and efficient enhanced forest resource inventories. The availability of high resolution digital imagery and LiDAR also enables the production of integrated resource inventories including topographic, hydrographic, vegetative, and ecosystem inventories that are well suited to supporting operational and strategic modelling applications. The focus of this project was on production of forest inventory attributes typically generated through the *ITC Suite* of software.

3.2. Individual Tree Crown (ITC) Approach

The Individual Tree Crown (ITC) Approach refers to a means of compiling forest information based on data derived from *individual trees* (or tree-clusters) within a forest through semi-automated analysis of multispectral digital imagery. Analysis of the input imagery consists of techniques for separating tree crowns from one another and from background vegetation, identification of tree species, grouping the delineated tree crowns into forest stands, and calculating stand level attributes based on aggregation of tree level information. Individual components of the overall approach have been programmed into a set of software tools and conveniently packaged as the *ITC Suite* of software (Gougeon and Leckie, 2003).

Details of the ITC Approach, including underlying assumptions are provided below in the Methods section (Section 4).

3.3. Research Partners

This project was implemented through the Forestry Research Partnership (FRP) with funding from the Enhanced Forest Productivity Science Fund, Tembec, the Canadian Forestry Services (CFS), and in-kind contributions from Ontario Ministry of Natural Resources (OMNR), Canadian Ecology Centre, and the CFS. Silvatech took on the task of running the *ITC Suite* of software on the data sets, identifying software issues, and producing this report. The team was led by Murray Woods (OMNR) and relied on François Gougeon (CFS) for technical advice about the implementation and improvement of the ITC software. Paul Courville (FRP) collected the field data which was crucial to the derivation of (grouped) species signatures. Dave Nesbitt provided compilation and database support. Don Leckie contributed to the overall design, made suggestions for the analysis and helped with field plot selection and data collection. Michael Chubey (Silvatech) carried out the brunt of the ITC analysis and reporting and identified issues for further investigation. Kevin Stehle (Silvatech) provided GIS support for the stand delineation and production of stand level ITC attributes as well as additional attributes. Geoff Lawless (Silvatech) provided manual Quality Control on the delineation results. Robert Albright (Silvatech) co-managed the project and contributed to the report.

The approach was very much a team effort with all partners contributing their expertise and energies to the project as appropriate. The highlight of the team's interaction was at the Enhanced Forest Inventory Workshop held at the CEC in Mattawa (May 22-24, 2007) where all partners presented results related to this project (<http://www.enhancedinventory.com>).

4. Study Area and Data

4.1. Location and description of study sites

Swan Lake Research Forest

The Swan Lake Forest Research Reserve is located 250 kilometres (km) north of Toronto and east of Huntsville, Ontario within Algonquin Provincial Park (Figure 1). The 2000 hectare (ha) site in Peck Township is located at 45 degrees (°) 28 minutes (') north (N), 78° 45' west (W), and ranges in elevation from 412 to 587 metres (m) above sea level. The reserve lies on the Pre-Cambrian Canadian Shield, with areas characterized by rolling hills and high rocky ridges that are separated by valleys scoured through glaciation. Outwash flats, ablation moraines, and drumlinoid deposits provide a range of soil depths that range from coarse to medium texture. The Algonquin Dome, due to its elevation, has a climate that is generally more cool and wet than the surrounding area (Cole and Mallory 2005).

The site is within the Great Lakes–St. Lawrence Forest Region and comprises mature stands of shade-tolerant and mid-tolerant hardwoods (hard [sugar] maple [*Acer sacharum* Marsh.], American beech [*Fagus grandifolia* Ehrh.], soft maple [*Acer rubrum* L.], yellow birch [*Betula alleghaniensis* Britt.], ironwood [*Ostrya virginiana* {Mill.} K. Koch]), conifers (eastern hemlock [*Tsuga canadensis* {L.} Carrière], white pine [*Pinus strobus* L.], white spruce [*Picea glauca* {Moench} Voss], red spruce [*Picea rubens* Sarg.] eastern larch [*Larix laricina* {Du ROI} K. Koch], eastern white cedar [*Thuja occidentalis* L.], balsam fir [*Abies balsamea* {L.} Mill.]), and minor proportions of mid-tolerant and intolerant hardwoods (white birch [*Betula papyrifera* Marsh.], black cherry [*Prunus serotina* Ehrh.], white ash [*Fraxinus americana* L.], black ash [*Fraxinus nigra* Marsh.], trembling aspen [*Populus tremuloides* Michx.]). Researchers have also established small spruce plantations from a variety of local, national, and international sources.

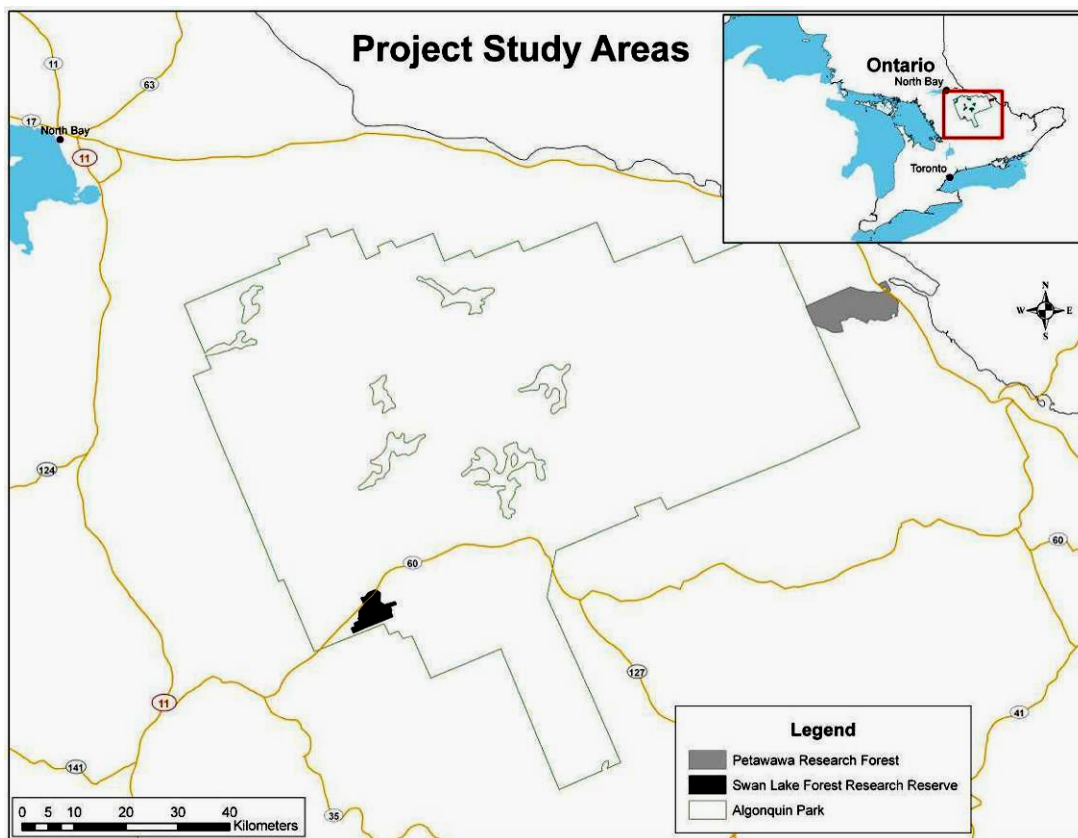


Figure 1. Map of study sites in Ontario.

Petawawa Research Forest

The Petawawa Research Forest (PRF) is located approximately 200 km west of Ottawa and 180 km east of North Bay, just east of Chalk River, Ontario (46° 00' N, 77° 26' W). The research forest encompasses 10,000 ha of mixed mature forest that is representative of the Great Lakes–St. Lawrence Forest Region and is characterized by eastern white pine, red pine, trembling aspen, and white birch. Red oak (*Quercus rubra* L.), dominates

many poor dry soils. Boreal forest species from the north and shade-tolerant hardwoods from the south exist on suitable sites.

PRF lies on the southern edge of the Precambrian Shield, with its topography strongly influenced by glaciation and post-glacial outwashing. There are three types of terrains characterizing the site: extensive sand plains of mostly deltaic origin; imposing hills, shallow, sandy soils and bedrock outcrops; and gently rolling hills with moderately deep, loamy sand containing numerous boulders. Elevations range from 140 to greater than 280 m above sea level within the forest. Mean annual precipitation for the research forest is around 82 centimetres per year. Approximately 25 percent (%) of the precipitation falls as snow. The mean annual temperature is 4.4° Celsius (C). The area averages 136 growing season days with an average of 100 days being frost-free.

4.2. Description of imagery and LiDAR data

Swan Lake

Imagery acquired on May 24, 2006 by M7 Visual Intelligence⁵ (M7VI) was used as the input data for the Swan Lake site. M7VI's sensor is a mosaicking 400 megapixel RGB and a separate 400 megapixel NIR system. The sensors are co-registered to create a multispectral data set. Imagery was acquired at 9500 feet (') above ground level resulting in a swath width of approximately 3 km and a pixel resolution of 33 cm. M7VI delivered orthophotos of the Swan Lake area in tiles spanning 2.5 x 2.5 km.

In addition, LiDAR data were collected simultaneously with the imagery using an upgraded Leica ALS40 airborne laser scanner mounted in a King Air 90 aircraft. The base mission was flown with a 20° field of view, scan rate of 30 hertz (Hz), and a maximum pulse repetition frequency of 32,300 Hz. This configuration resulted in a cross track spacing of 2.87 m, an along track spacing of 2.4 m, an average sampling density of 0.46 points m⁻², and a swath width of approximately 1 km. The LiDAR point cloud data were classified as ground or vegetation by the vendor using proprietary algorithms.

Petawawa Research Forest

Imagery acquired through First Base Solutions⁶ was used as the input data for the Petawawa site and combined with LiDAR data (described above) collected by M7 Visual Intelligence. The Vexcel Ultracam sensor provided 28 cm RGB and NIR imagery collected in August 2006 and later post-processed into 40cm/pixel orthophotomosaics by First Base Solutions using the PCI OrthoEngine, which implied automatic colour balancing and automatic outline determination. In addition, manual cloud and cloud shadow removal was performed and the data replaced by patches from other flight lines.

⁵ M7 Visual Intelligence- 510 Bering Dr., Suite 310, Houston, TX, USA 77057

⁶ First Base Solutions -140 Renfrew Drive, Suite 100, Markham, Ontario, Canada L3R 6B3

4.3. Description of field data

A range of tree species communities were present on each study site. Tables 1 and 2 list the species that were sampled to support the development of spectral signatures for their prediction across the inventory area. Five methods of training for spectral signatures were utilized in this project (described in Section 5). Methods 1 to 3 required the collection of spatial species coordinates based on ground sampling. To support this spatial species coordinates were collected for the range of tree species on the two sites during the period of April 2006 to July 2007. At the Swan Lake Research Reserve, 576 trees were spatially sampled representing the fifteen tree species listed in Table 1. Petawawa Research Forest had 620 tree spatial coordinates collected representing the nineteen tree species listed in Table 2. All points were collected using a Trimble Pro XT kinematic GPS with a Hurricane antenna. In addition, 40 other sites containing multiple trees of the same species were located and manually positioned on the imagery and were available for use with Methods 4 and 5 of training and signature generation.

Table 1. Tree species sampled at the Swan Lake Research Forest.

| Common tree species name | Scientific tree species name | Abbreviation |
|----------------------------|---|--------------|
| American beech | <i>Fagus grandifolia</i> Ehrh | Be |
| balsam fir | <i>Abies balsamea</i> (L.) Mill. | Bf |
| black cherry | <i>Prunus serotina</i> Ehrh | Cb |
| Eastern white cedar | <i>Thuja occidentalis</i> L. | Ce |
| Eastern hemlock | <i>Tsuga canadensis</i> (L.) Carr. | He |
| ironwood | <i>Ostrya virginiana</i> (Mill) K. Koch | Id |
| red maple | <i>Acer rubrum</i> L. | Mr |
| red pine | <i>Pinus resinosa</i> Ait. | Pr |
| sugar maple (hard maple) | <i>Acer saccharum</i> Marsh | Mh |
| white birch | <i>Betula papyrifera</i> Marsh | Bw |
| white pine | <i>Pinus strobus</i> L. | Pw |
| white spruce | <i>Picea glauca</i> (Moench) Voss | Sw |
| yellow birch | <i>Betula alleghaniensis</i> Arnold | By |
| Colorado blue spruce | <i>Picea pungens</i> Engelm | Sc |
| red spruce | <i>Picea Rubens</i> Sarg. | Sr |
| Ezomatsu (Japanese) spruce | <i>Picea jezoensis</i> Carr. | Sj |

5. Methods

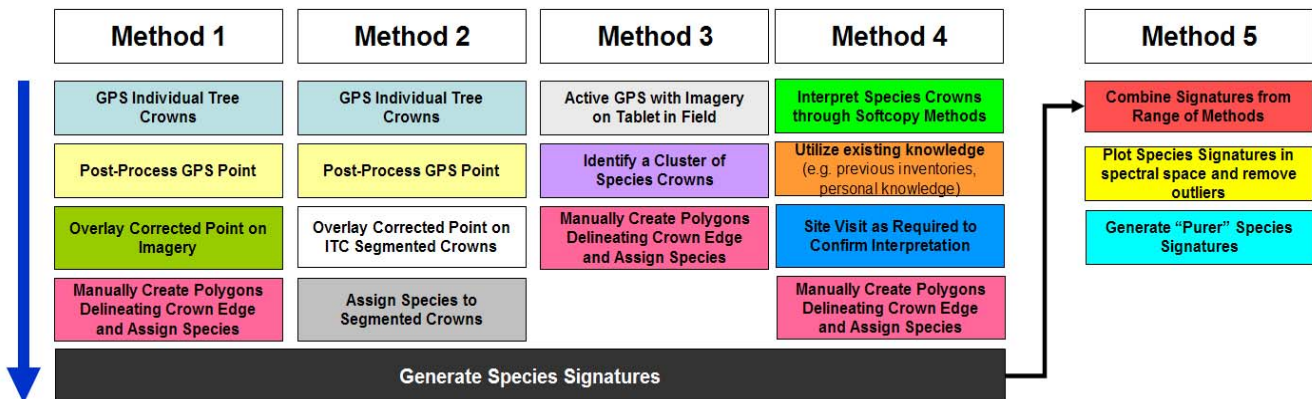
This section describes the methods followed for the field data collection as well as the data analysis procedures implemented in the *ITC Suite* production run.

Table 2. Tree species sampled at the Petawawa Research Forest.

| Common tree species name | Scientific tree species name | Abbreviation |
|--------------------------|---|--------------|
| American beech | <i>Fagus grandifolia</i> Ehrh | Be |
| white ash | <i>Fraxinus Americana</i> L | Aw |
| black ash | <i>Fraxinus nigra</i> Marsh | Ab |
| basswood | <i>Tilia Americana</i> L. | Bd |
| balsam fir | <i>Abies balsamea</i> (L.) Mill. | Bf |
| white birch | <i>Betula papyrifera</i> Marsh | Bw |
| yellow birch | <i>Betula alleghaniensis</i> Arnold | By |
| Eastern hemlock | <i>Tsuga canadensis</i> (L.) Carr. | He |
| ironwood | <i>Ostrya virginiana</i> (Mill) K. Koch | Id |
| tamarack | <i>Larix laricina</i> (Du Roi) K. Koch | La |
| sugar maple (hard maple) | <i>Acer saccharum</i> Marsh | Mh |
| red maple | <i>Acer rubrum</i> L. | Mr |
| red pine | <i>Pinus resinosa</i> Ait. | Pr |
| white pine | <i>Pinus strobus</i> L. | Pw |
| jack pine | <i>Pinus banksiana</i> Lamb. | Pj |
| trembling aspen | <i>Populus tremuloides</i> Michx. | Pt |
| black spruce | <i>Picea mariana</i> (Mill.) BSP | Sb |
| white spruce | <i>Picea glauca</i> (Moench) Voss | Sw |
| red spruce | <i>Picea Rubens</i> Sarg. | Sr |

5.1. Field data collection and classifier training methods

Combinations of five variations of similar methods were employed to collect and utilize the training data necessary for classifying tree species. A description of each method employed is presented below. Figure 2 presents the methods and their relationships.



* Common Steps Colour Coded

Figure 2. Species training methods.

5.1.1. Method 1

Field crews collected GPS points for the range of species occurring in each of the study sites. For each tree, the hurricane antenna of the GPS was positioned as close as possible to the centre of the tree crown (Figure 3) and point data was collected for 30 second durations to permit post processing to sub-metre accuracy. The collection period for this dataset was between June and August 2006 and represented the sampling of 107 tree crowns (nine species) in Swan Lake and 64 tree crown (15 species) locations in Petawawa Research Forest. A polygon ESRI shapefile was then manually created to delineate tree crowns of the recorded species. These polygon shapefiles were used as training sites for *ITC Suite* (Figure 4) spectral signature derivation.



Figure 3. Recording the centre of a tree crown in Swan Lake with the Trimble ProXT and Hurricane antenna on a 'ruggedized' laptop.

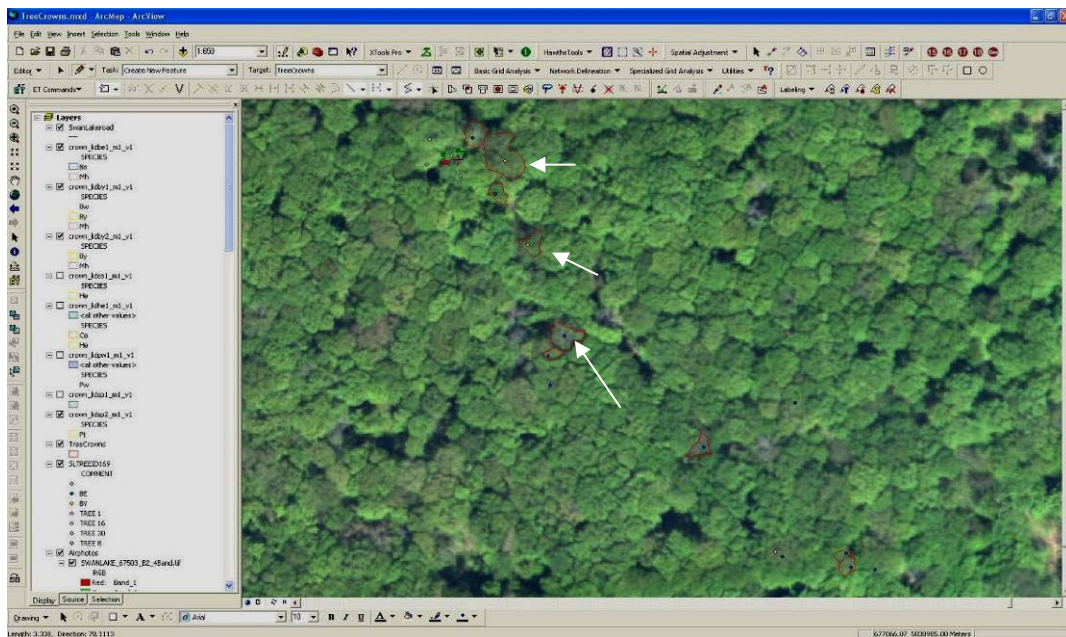


Figure 4. Creating tree crown polygon from GPS positional information.

5.1.2. Method 2

Method 2 followed the same collection methodology as Method 1.

106 points were collected in the Swan Lake Research Reserve and 137 in the Petawawa Research Forest, but only 66 of the 137 collected in PRF were used due to GPS accuracy issues. The collection period for this dataset was March 2007 for Swan Lake and April 2007 for the Petawawa Research Forest. Instead of providing manually delineated crown outlines based on the GPS position and recorded species, these points were overlaid on the segmented crown polygons created at an earlier step in the ITC process. Species were assigned to the segmented crown polygon where the two intersected.

5.1.3. Method 3

Method 3 involved a shift from collecting individual tree crown spatial location to focusing more on clumps of crowns for a given species. A tree clump was characterized by three or more crowns adjacent to each other with no interruption by another tree species (Figure 5).

Differing from the previous two methods, digital imagery on a tablet computer in the field was used as the means of identifying tree crowns for GPS data collection. The imagery that was to be used in the *ITC Suite* was uploaded to the data-logger and used for location information. Using the visual aid of the data-logger, a GPS point was created manually on the crown of interest. No post processing of the GPS point was required as the GPS point recorded was verified to its location visually on the imagery as demonstrated in Figure 5. The GPS points were then used to produce tree species crown

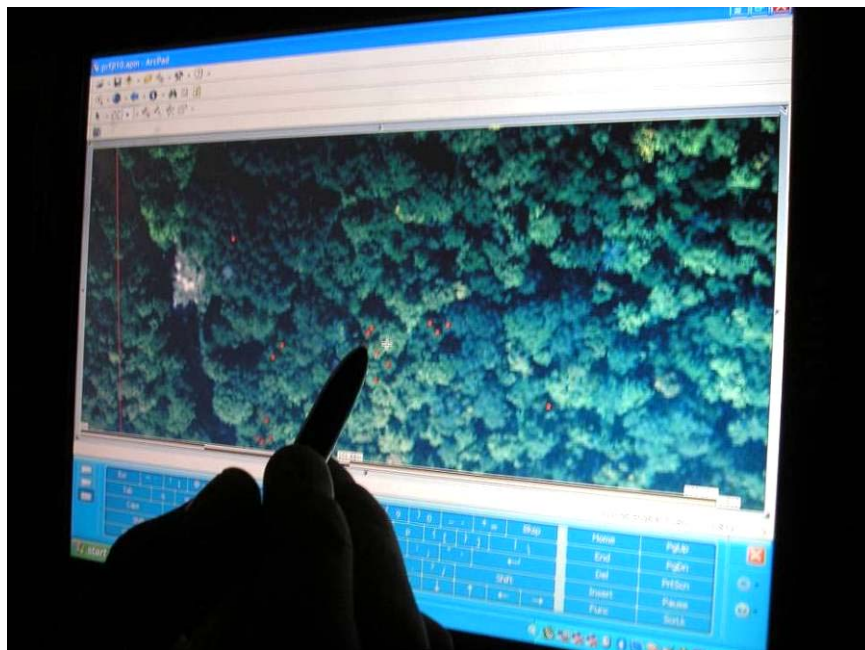


Figure 5. Identifying and marking points on clusters of tree crowns on the data tablet in the field as used in Method 3.

polygon shape files as in Method 1.

At Swan Lake, 363 GPS points were collected which helped create 125 tree clump polygons representing 9 tree species. At the Petawawa Research Forest, 419 GPS points were collected which helped create 163 tree clump polygons representing 17 tree species. The collection period for this dataset was between June and July 2007.

5.1.4. Method 4

Method 4 is a much more ‘production-oriented’ approach. It does not concentrate on precise field work, relying on quick site visits only when needed. It is essentially relying on the interpretive skill, experience and resourcefulness of the image analyst in a soft-copy environment.

The method consists of getting familiar with the territory via its imagery and trying to perceive the subtle differences between ‘the look’ of the different species on the image. To hone his/her interpretive skills, the analyst can rely on all kinds of auxiliary data such as: the most current (yet old) forest inventory, historical aerial photos, base maps, and even Google Earth views of the area. The analyst should also create an image enhancement that shows species differences beyond the traditional panchromatic, RGB or CIR views, making good use of the multispectral nature of the data. Once such enhancement is arrived at, lookup tables are created and saved to make sure the colour enhancement will be consistently the same independent of scale (i.e., many image display software systems have adaptive colour display capabilities trying to optimize contrast, brightness, etc. for specific views of the data, and thus make a different use of the colour space depending on the content of the displayed part of the image).

Once familiar with the look of the different species throughout the imagery, the user delineates sizeable (50-200 trees) single species areas on the screen, assessing species by interpretation and/or the use of auxiliary data (Figure 6). Only areas that are significantly distinct in colour, texture, or structure from each other are selected. If the species remains unknown, then a visit to the site is warranted, not only to assess the species of such cluster of trees, but also to ascertain that it indeed consists of a single species. For the sake of efficiency, one should make sure that these areas are easily accessible and once there, that the tree clusters are easy to locate in the field. Here, the field crew was supplied with overview images and GPS locations to facilitate locating the tree clusters and close-up views of the tree cluster to record any anomalous trees on the image.

For tree species that do not grow in clusters and that are hard to identify otherwise, one must rely on the previous methods of field data acquisition. However, unless it’s a very valuable species or some kind of indicator species, one must consider if such ‘field sorties’ are warranted, especially considering that knowing about such species may not make much difference to the overall forest inventory of the region.

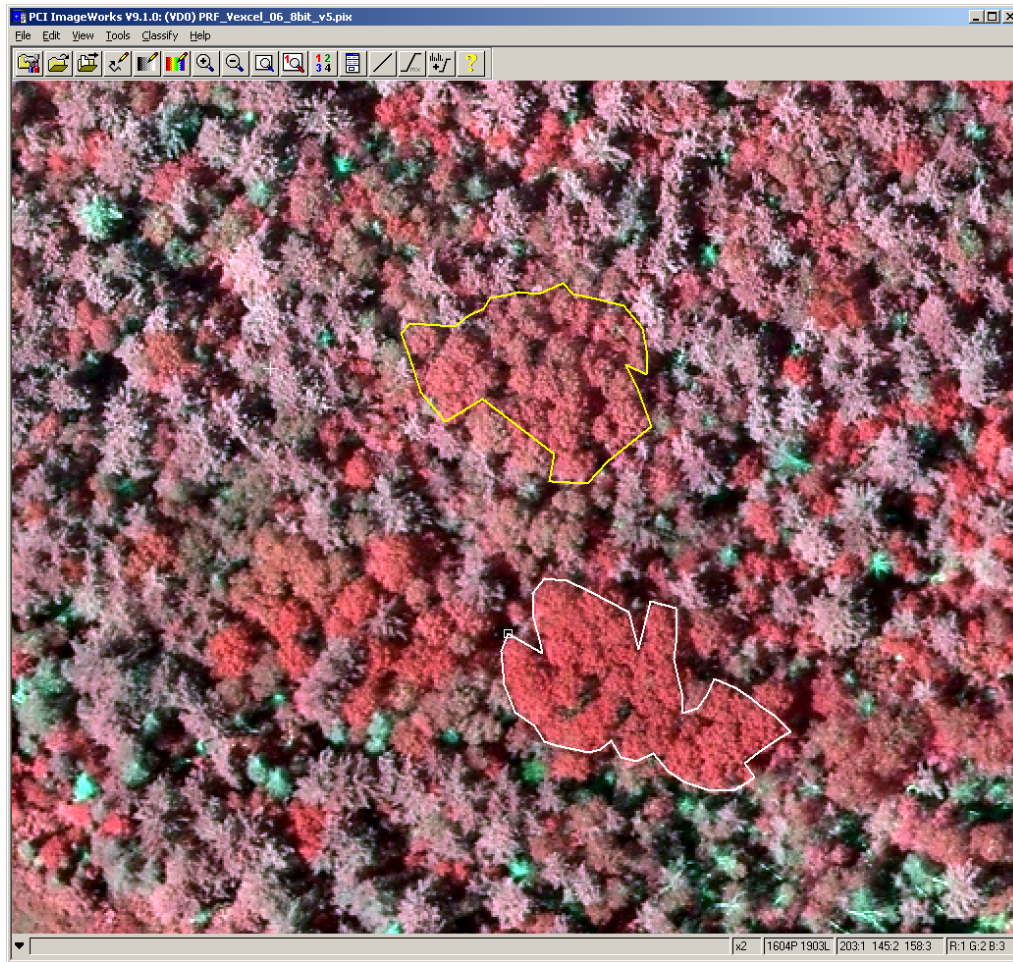


Figure 6. Examples of sizeable single species areas delineated on the screen in the fourth method of signature acquisition.

5.1.5. Method 5

Method 5 consisted of judiciously combining the signatures of the ITCs from the training areas in Method 4, with some of the individual tree crown manually delineated in Method 1 and 2, and some improved clusters from Method 3, to generate the species signatures. In addition, these individual tree signatures were plotted in spectral space (see Figure 7) and obvious outliers were removed to create tighter ('purer') signatures.

When obvious natural variations existed within a given species, the trees of that species were separated into two or three classes. For example, Figure 8 shows why the larches were broken into two classes, named normal larch (La nm) and bright larch (La br). Similar situations led to three white pine classes (old, immature, bright), two types of white birch (normal and damaged), and two types of trembling aspen (normal and poor quality). This led to signatures with fairly good separability, as illustrated by Figures 9 and 10.

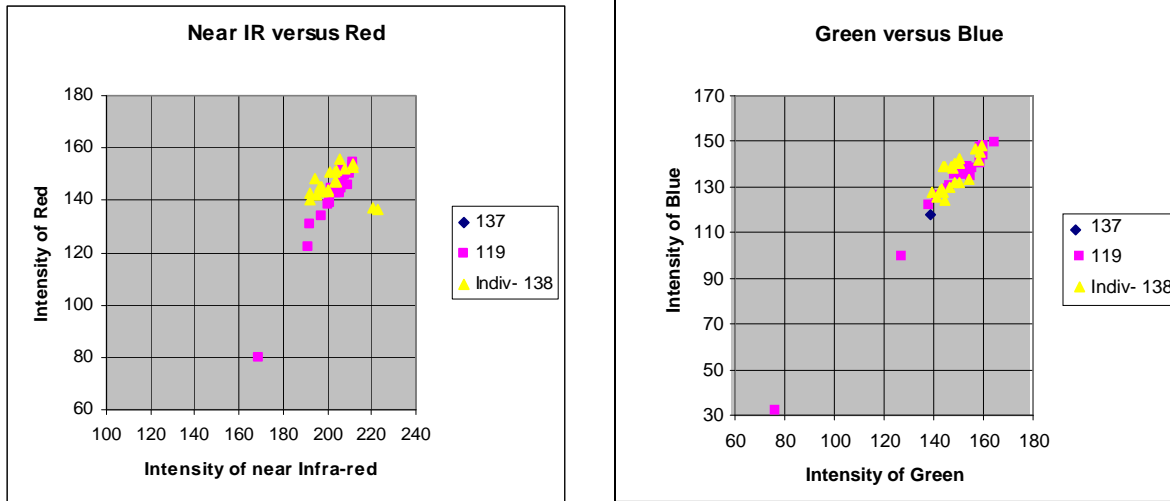


Figure 7. Plots of individual tree crowns of large toothed aspen (Alt) from three training sets making obvious the outliers to be removed in order to purify the signature.

The ITC analysis was confined to a sub area (7 km x 8 km) of the Petawawa Research Forest where the combination of the automatic colour balancing (done by the data supplier) and our image normalizations (in two directions, as surrogate for radial corrections) appeared to have worked better (even though a sizable portion of that area [lower centre] was also obviously not well balanced, see Figure 11). The use of a smaller area allowed us (in view of Windows XP user-useable limit of 3GB) to introduce the blue spectral band in the signature generation and classification processes.

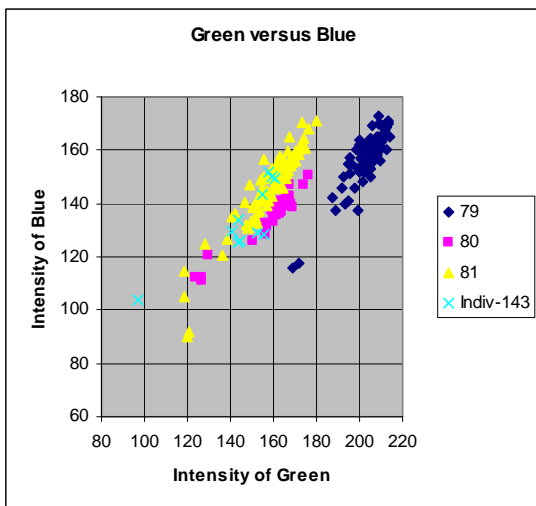


Figure 8. Plots of individual tree crowns of larch from four (4) training sets making obvious why larch crowns were broken into two classes, later named normal larch (La nm) and bright larch (La br).

5.2. Data analysis methods

5.2.1. Introduction

The methods applied in this project consisted mainly of a series of image analysis techniques known collectively as the *ITC Approach* (Gougeon, 1995). Most of the components of the approach are available as a series of software tools within the *ITC Suite* (Gougeon and Leckie, 2003). Part of the mandate of this project was to apply the *ITC Suite* in a simulated production environment to evaluate the viability of the ITC approach for operational use in large-scale forest resource inventories using aerial data. To this end, it was necessary to augment the overall approach in order to address some of the challenges typical of an operational setting and large data volumes.

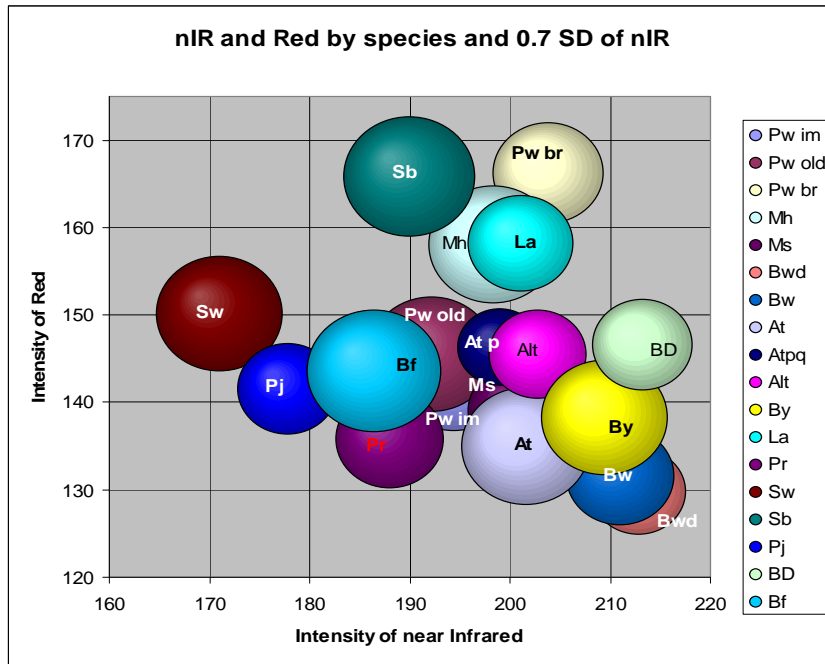


Figure 9. Plot of signatures in multispectral space (near infrared vs. red) illustrating the potential separability of classes (or lack thereof) from this particular point of view.

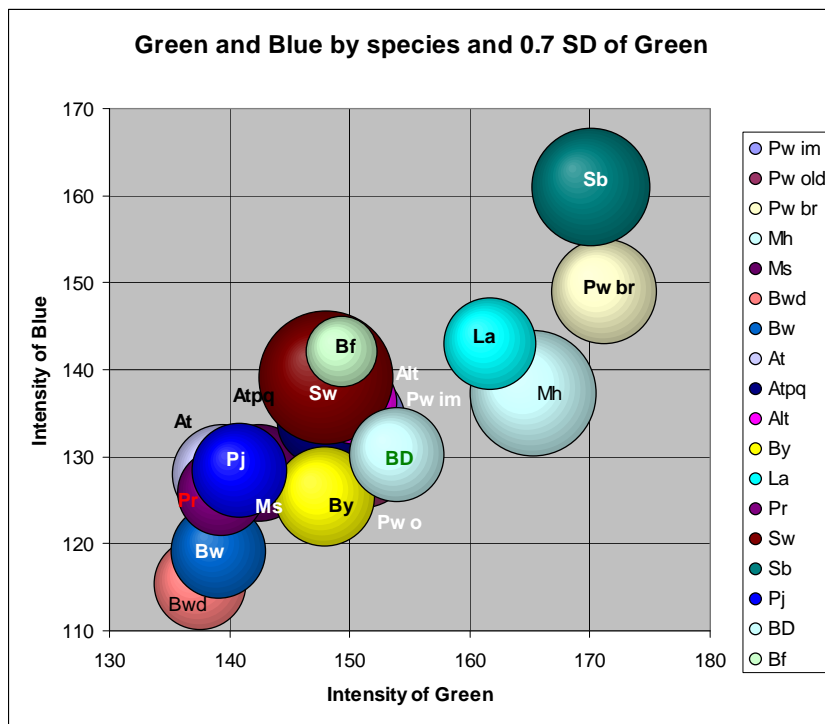


Figure 10. Plot of signatures in multispectral space (green vs. blue) illustrating the potential separability of classes (or lack thereof) from this particular point of view.

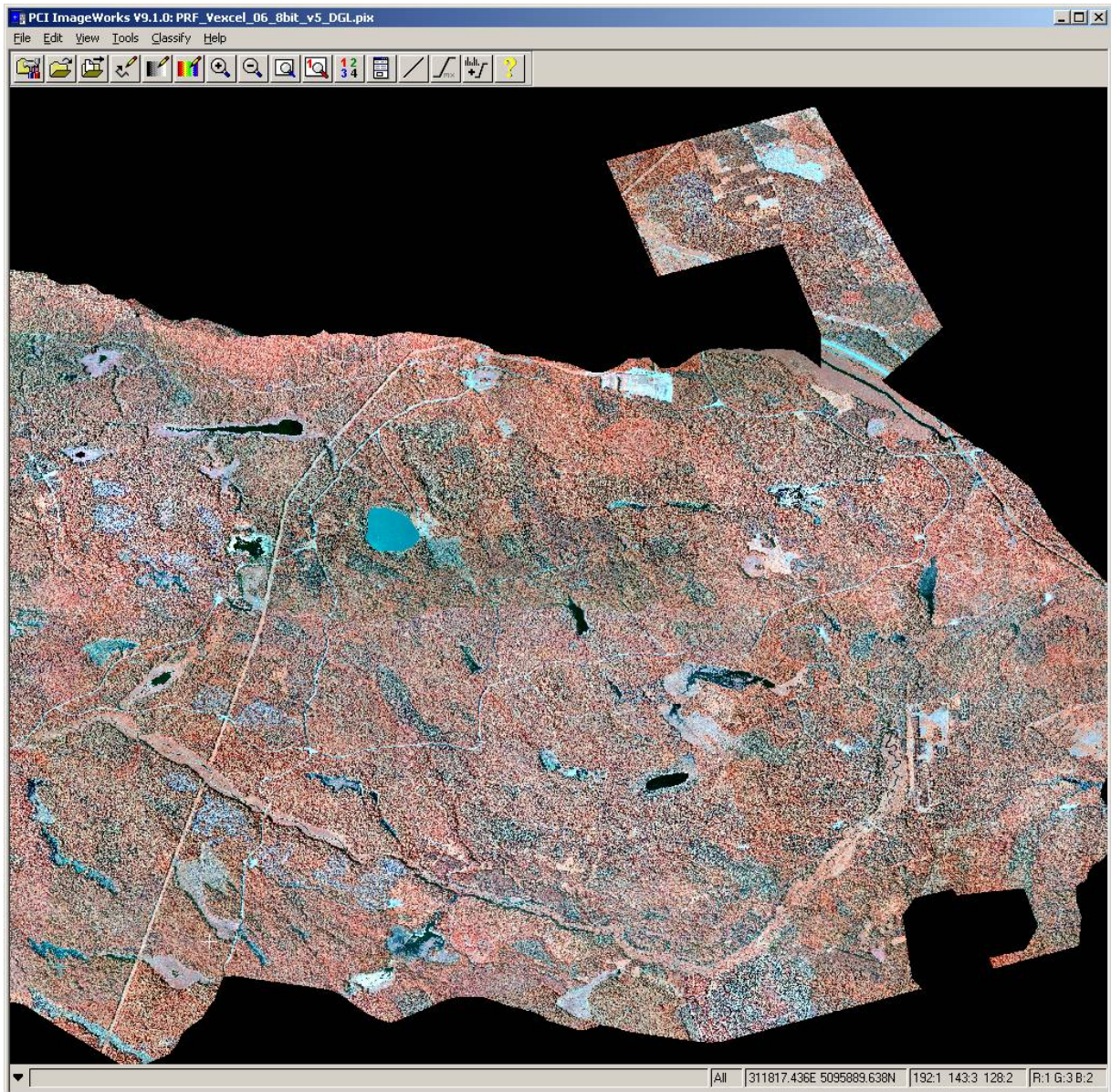


Figure 11. Sub-area (7 km x 8 km) of the Petawawa Research Forest supplied orthomosaic as used with Method 5. Even after substantial Bidirectional Reflectance Distribution Function (BRDF) and normalization efforts, the image still exhibits how some parts of the area appear relatively well-balanced radiometrically while other parts (low centre) appear normalized different.

Use of frame based aerial imagery over large areas also presents some additional issues such as the large quantities of discrete images or orthophoto tiles from the airborne sensors, and the spectral inconsistencies within and among those images (see Appendix 1 for a discussion of these issues).

5.2.2. *Operational Considerations*

The main operational related challenges considered in this project were those associated with scale. A typical forest inventory in Canada can cover several hundred thousand hectares of forest, requiring thousands or tens-of-thousands of image tiles. The only economically viable way to process such vast volumes of data is through automation. Consequently, the various steps within the processing chain were programmed into batch processing scripts wherever possible. A major challenge of working with multiple adjacent image tiles is the issue of image spectral consistency between and within tiles. This issue was addressed through the development of an image normalization procedure as described below.

5.2.3. *Preliminary Image Processing*

Use of frame based aerial imagery requires processing beyond what is needed for satellite image based ITC analysis or even that for linear array airborne imagery. Solutions to issues with linear array images have been developed and applied on small study areas. These issues are magnified using frame based systems and large operational trials. The imagery was prepared for analysis through a preliminary processing phase consisting of masking, view angle correction and image normalization. The preliminary processing workflow is depicted in Figure 12 and outlined below in sections 5.2.3.1 and 5.2.3.2.

5.2.3.1. *LiDAR-Based Masking*

Forest canopy and non-forest area masks were generated based on a combination of image spectral thresholds and elevation information derived from the co-registered LiDAR data set. The masks were required inputs for the image normalization process as well as for several of the *ITC Suite* programs.

This project identified that LiDAR information was important to the development of accurate forest/non-forest masks. A digital canopy height model (CHM) was used to identify non-forested areas based on LiDAR-derived height-from-ground data. Non-forest was defined as pixels with CHM values of < 3 metres. Examples of the masking output, including a comparison of a LiDAR-based mask versus an ‘image-only’ mask, are presented in the Preliminary Results and Discussion chapter (Section 6).

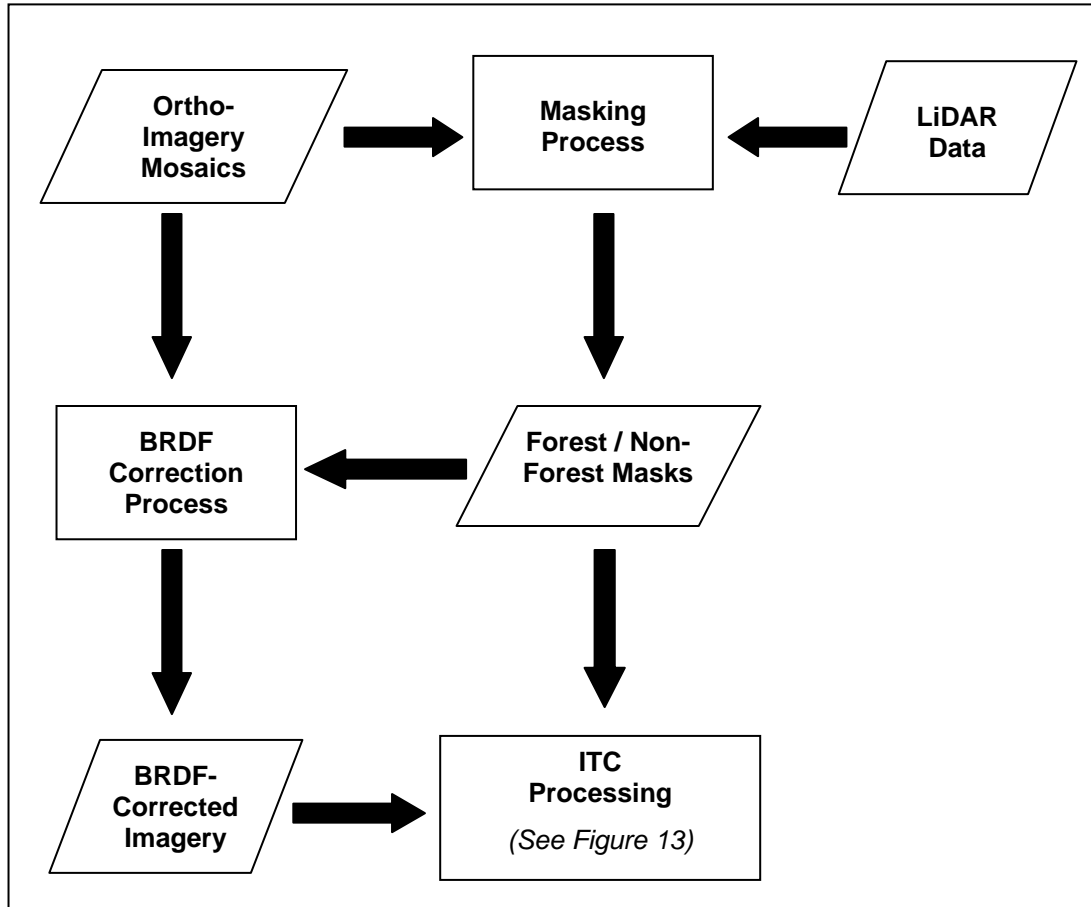


Figure 12. Preliminary processing workflow.

5.2.3.2. BRDF Correction – Image Normalization

An attempt was made to account for different sun-object-viewer geometry within the imagery and normalize the original image data using a Bidirectional Reflectance Distribution Function (BRDF) correction procedure. The goal of the BRDF correction was to improve the overall radiometric consistency of the image data sets by correcting for the relative radiometric differences between and within image tiles associated with the large view angles of aerial sensors and the sun angles at the time of data acquisition. It was also hoped that a normalization factor in the BRDF program could be used to compensate for the colour balancing performed by the image producers during the creation of orthophoto tiles from the digital photos. Of course, without very specific information, nothing could be done to compensate for the manual patching (i.e., cloud and cloud shadow removal) done by one of the image providers (First Base Solutions). Certain ‘features’ specific to the M7VI sensor (i.e., the wide push broom approach) and to the Vexcel Ultracam sensors (i.e., a nine section panchromatic image) could not be compensated for either (see Appendix 1). BRDF correction was applied using an optional *ITC Suite* program (modified specifically for this project by F. Gougeon) called *MFPWBRDF* (Multi-Feature Piece-Wise BRDF Correction).

5.2.4. ITC Suite Processing

The ITC processing chain has been well-documented elsewhere (e.g. Gougeon, 1995, 1997; Gougeon and Leckie, 2003, 2006) so will only be outlined briefly here. The core components of the ITC approach consist of delineation and classification of individual tree crowns (Figure 13) followed by grouping the classified crowns into forest stand polygons (Figure 14).

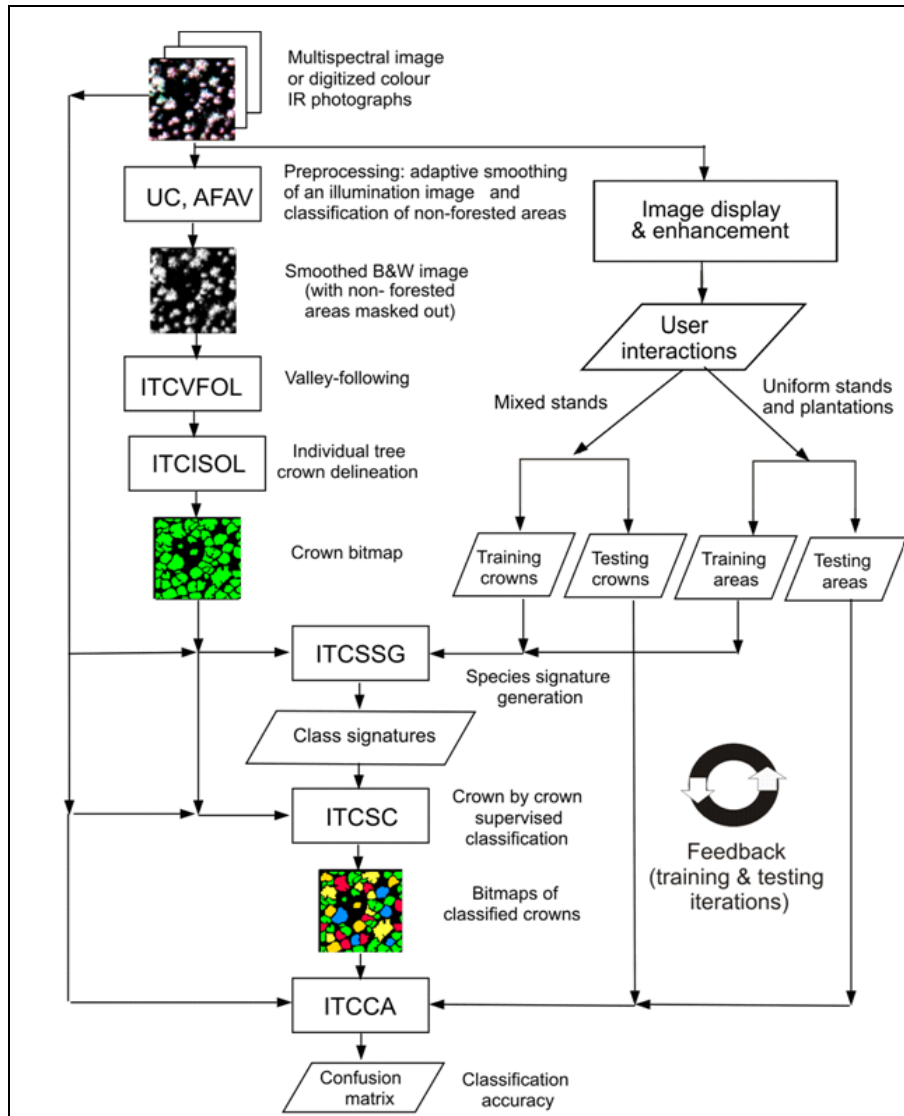


Figure 13. ITC approach workflow: individual tree crown delineation and ITC approach workflow: individual tree crown delineation and classification (based on Gougeon, 1997).

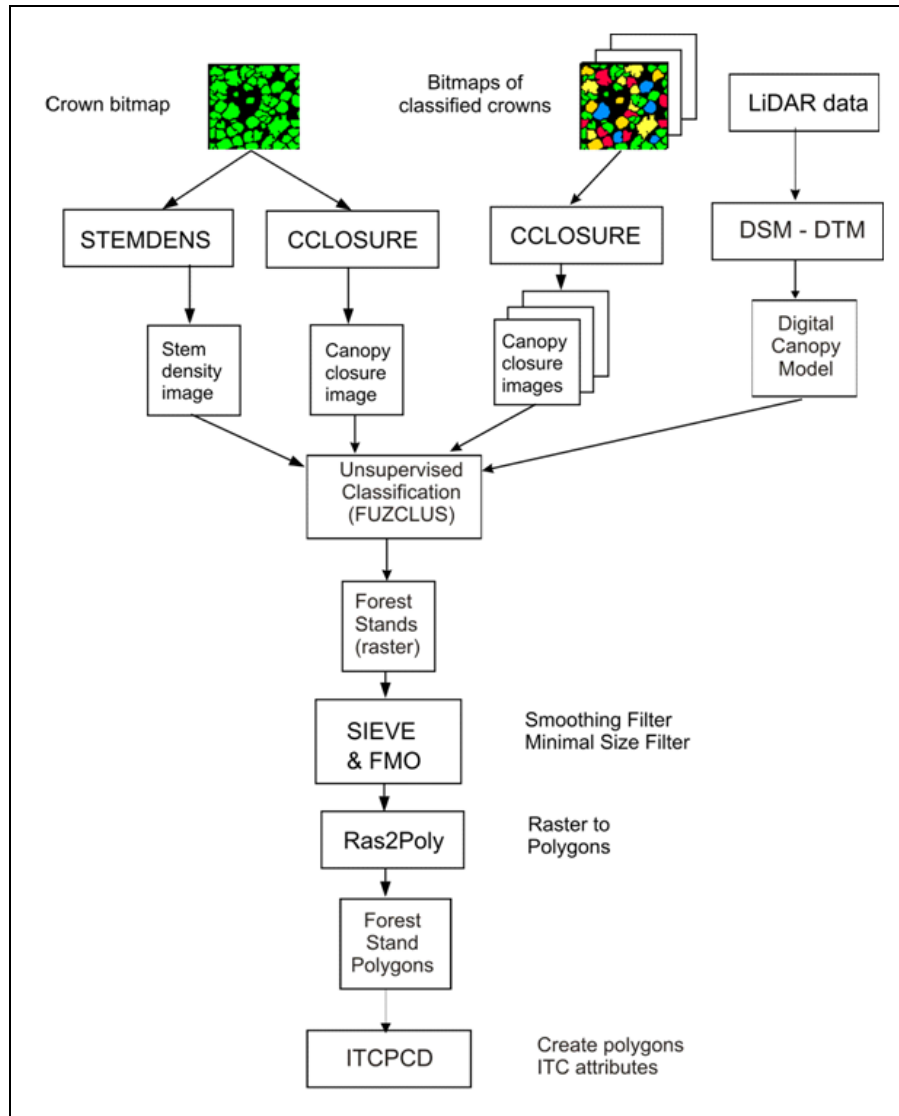


Figure 14. ITC approach workflow: forest stand polygon delineation (based on Gougeon, 1997).

Tree crown delineation is a two-part process. Initially, a ‘valley following’ operation (*ITCVFOL*) locates local minima, or dark pixels within the shaded portions of the image, and systematically follows the valleys of shade between trees throughout the image. Secondly, a rule-based isolation process (*ITCISOL*) is used in conjunction with the ‘minima network’ from the valley following output to delineate the perimeters of individual trees and tree clusters. A non-forest mask (generated at the preliminary processing stage outlined in Figure 12) is used to constrain the valley following and crown isolation algorithms to areas occupied by the forest canopy.

The *ITC Suite* classification tool (*ITCSC*) is based on a supervised classification approach where delineated tree crowns are classified by species according to a maximum

likelihood rule using spectral signatures generated from training samples. Training samples collected through fieldwork or by image interpretation (as described in the Methods section) and species signatures were generated using the *ITCSSG* program. The optional *ITC Suite* program, *ITCSSBD* (ITC Species Signature Bhattacharyya Distance), was used for statistical evaluation of the species signatures separability.

Grouping of classified tree crowns into forest stand polygons was achieved through unsupervised clustering of a series of pseudo images derived based on species class, crown closure and stem density characteristics, as illustrated in the process outlined in Figure 14.

Several additional forest resource attributes were generated using *ITC Suite* tools not depicted in the ‘standard’ ITC workflow shown in Figures 13 and 14. These include identification of local maxima representing the tops of individual trees (useful for calculating simple tree counts) using the *TREETOPS* program, and generation of within-stand-polygon summaries of various attributes (e.g. polygon area, number of crowns by species, crown closure, stems/ha, etc.) using *ITCPCD* (ITC Polygon Content Description).

5.2.5. *Post-Processing*

The automated forest stand delineations were imported to ArcGIS™ and subjected to a smoothing algorithm prior to manual editing of the line work. Editing consisted of general ‘cleaning’ of the automated polygons and ‘edge matching’ at boundaries of adjacent image tiles (the latter only required if automated polygons are developed on a tile by tile basis). Finally, an ArcGIS™ database was constructed and populated with ITC forest polygon attributes calculated through aggregation of the individual tree crown data using *ITCPCD*.

5.2.6. *Production Times*

This section summarizes the main tasks in the ITC production run and the time required under typical conditions.

5.2.6.1. *Field Data Collection and Classifier Training Time Requirements.*

The spatial recording of training sites for Methods 1 to 3 was carried out in three field trips. Collection of coordinates was carried out in leaf-off and leaf-on conditions. Table 3 outlines the time required to physically travel between the crowns and record the positions after driving to the research site, post-processing the coordinates where required and delineating crown polygons.

Table 3. Time requirement for training site data collection

| Training Site Collection Method | Total Time (minutes) | Crown GPS positions at Swan Lake Research Forest | Crown GPS positions at Petawawa Research Forest | Average Time per Tree Training Site (minutes) |
|---------------------------------|----------------------|--|---|---|
| 1 | 2400 | 107 | 64 | 14 |
| 2 | 3360 | 106 | 137 | 13.8 |
| 3 | 5400 | 363* | 419** | 6.9 |

* resulted in 125 tree clump polygons for Swan Lake

**resulted in 163 tree clump polygons in the Petawawa Research Forest.

Methods 4 and 5 involved the use of skilled interpreters delineating polygons of similar species for training purposes. This approach is interactive and the amount of effort required to sample with this method is a function of the species and age/site class variability. For the Petawawa study site, 40 sites were identified for field checking. Two were eliminated during the field assessment; one had too many trees of different species and a second was too difficult to precisely locate the trees of interest. The field work was conducted over three days and took on average approximately 25 minutes per site. Sites contained approximately 5–30 trees each. Approximately 500 trees were checked. The ITCs within them were generally used for training but some manual interpretation and delineation of trees was also done (one day).

5.2.6.2. *Image Preparation and Processing*

The total time required for the image preparation and processing was difficult to track as there were many issues which interrupted the workflow. Reflecting back on the process and knowing what we know now the following is a proportional breakdown of the effort required in the various stages of the ITC process.

| | |
|---------------------------|-----|
| Imagery prep | 20% |
| Tree crown delineation | 20% |
| Species classification | 40% |
| Stand polygon delineation | 20% |

It has been a challenge to quantify the time required in terms of weeks per map sheet or days per kilometre squared ($/\text{km}^2$) in a meaningful way. Summarizing the time inputs required for the production of semi-automated outputs in this manner would be misleading when extrapolated to larger areas. Figure 15 is an attempt to illustrate that with the ITC approach to producing the raw inventory attributes, there is an up front investment in time required to set up and calibrate the process with the available input data. The larger the area, the more significant the gains in productivity are expected to be, as the fixed effort will be amortized over larger areas and a larger area can be run through the semi-automated classification processes. The minimum area threshold where the ITC approach crosses the current soft-copy methods is unknown at this time.

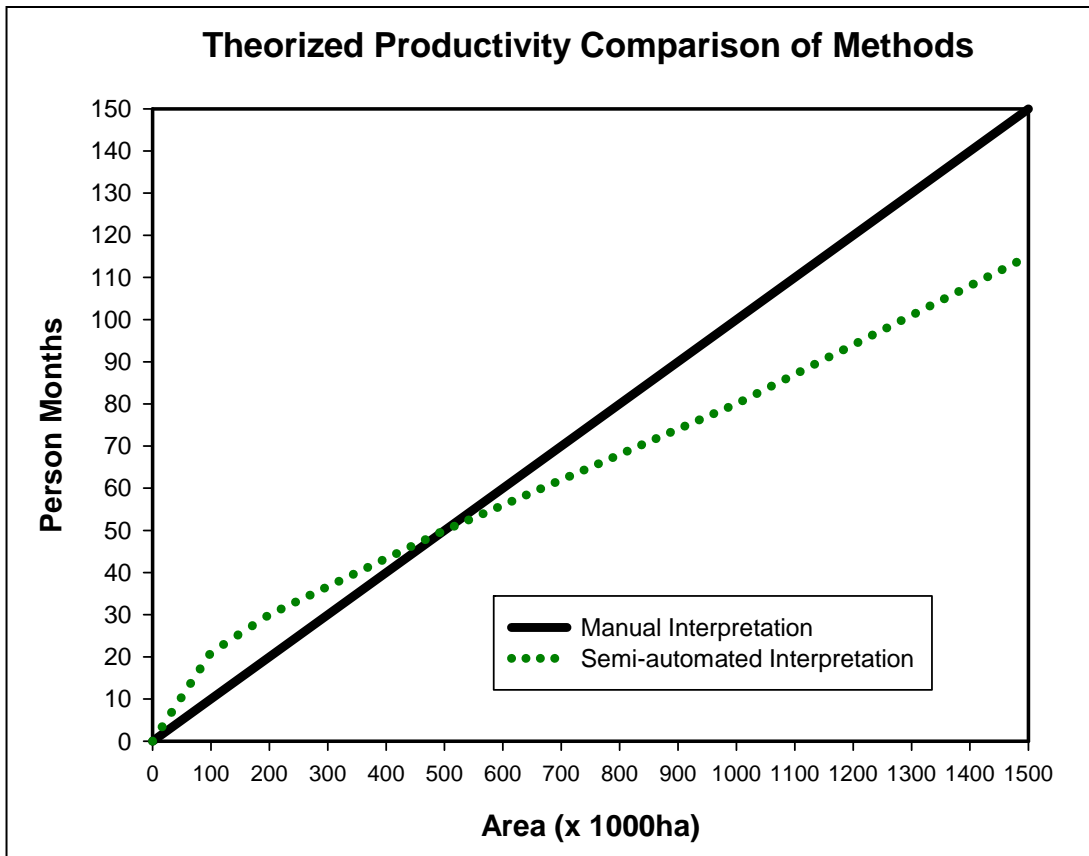


Figure 15. Theorized manual and automated productivity comparison.

5.2.6.3. Manual Editing of Stand Delineation

The effort required to produce stand boundaries is estimated to be approximately 2–4 hours per 100 sq km depending on the complexity of the forest and the final inventory requirements in terms of polygons per map sheet and minimum and maximum polygon sizes.

5.2.6.4. GIS Operations to Populate Database

Some effort is required to create algorithms which populate the spatial database linked to the polygons to the desired inventory format. Once the programming is completed however the process is fully automated and no further effort is required. Related to the point in 5.2.6.2 the larger the area that can be processed the larger the gains in efficiency will be as the initial effort to ensure the integrity of the database is amortized over a larger area.

6. Preliminary Results and Discussion

6.1. Introduction

This section of the report provides a mainly qualitative assessment of the ITC analysis results, and does not, as yet, address the ITC outputs in quantitative terms (hence the section title ‘Preliminary Results ...’). Quantitative assessment of classification accuracy will be performed and documented in a subsequent report. From the outset of this project the intention was to produce stand level attributes based on tree level information, and therefore to assess the results at the stand level. Although full automation of much of the ITC processing chain was achieved as a result of this project, stand delineation still requires a final manual editing stage because the ITC analysis was always carried out on subsets on the full area. In order to keep the manual component to a minimum, it was decided to limit the stand delineation to specific validation areas on each of the two project sites. The validation areas consisted of two of the 2.5x2.5 km Swan Lake image tiles, and 20 of the 1x1 km Petawawa tiles. The 20 Petawawa tiles were mosaicked prior to analysis in order to reduce the need for manual edge matching.

6.2. Tree Crown Delineation

As described in the Methods section, tree crown delineation using the ITC approach relies on the appearance of shade ‘valleys’ between trees in the input imagery. This condition is most consistently met in stands of mature conifer (softwood) trees. Deciduous (hardwood) stands, on the other hand, usually have larger, rounder crowns that tend to inter-mingle with each other, leading to less distinct or even non-existent valleys of shade between trees. In addition, deciduous trees have multi-lobed crowns that may lead to over-segmentation into separate stems in some cases. Consequently, delineation of *individual trees* is generally more likely in conifer stands while delineated ‘crowns’ in predominately deciduous stands are often best described as *tree clusters* rather than individual trees. Overall, the delineation output for both sites consisted of both individual trees and tree clusters (Figure 16).

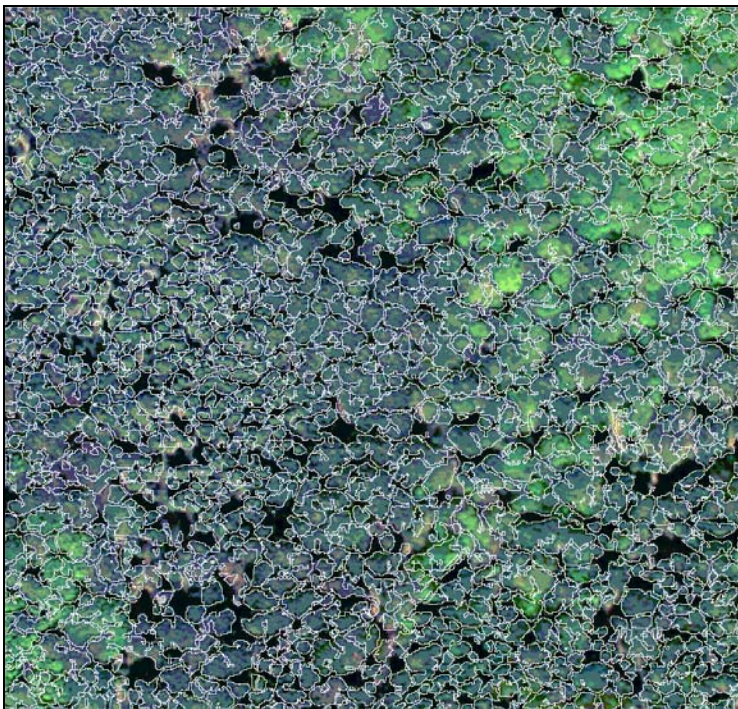
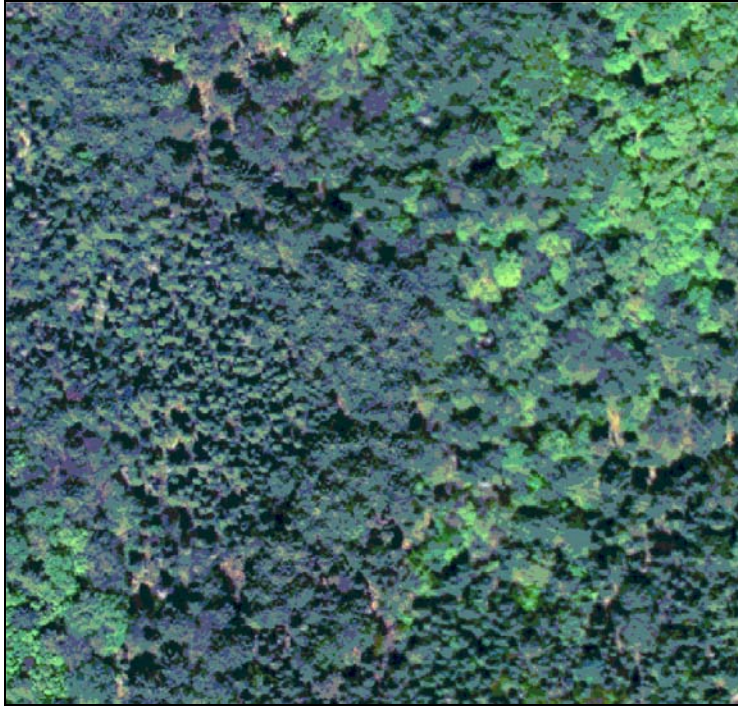


Figure 16. ITC delineation example (Swan Lake); scale = 1:1,000.

6.3. Species Classification

6.3.1. Swan Lake Species Signatures and Classification with Methods 1 - 3

Classification of tree crowns at the Swan Lake site was performed using signatures from eight species (Be, Bf, By, Ce, He, Mh, Pw, Sw) derived from training data gathered from three image tiles (67503_C4, 67503_D4, 67504_A4). A statistical evaluation of species signature separability among the final eight signatures is presented in Table 4. This summary of species separability was generated using the *ITC Suite* program *ITCSSBD* (ITC Species Signature Bhattacharyya Distance) which calculates the pairwise separability (Jeffries Matisuta Distance) of signatures of each possible combination in the input signature list. *ITCSSBD* separability measures yield values between 0 and 2, where 0 indicates complete overlap between the signatures of two classes, and 2 indicates a complete separation between the two classes. Values below 1 indicate very poor separability (the two signatures are statistically very close to each other), while values greater than 1 indicate that the two signatures are separable to some extent (the higher the value, the greater the separability). Originally, the training data set included two additional species (Cb, Mr); however, Cb was dropped from the analysis due to a very small number of samples, and the two maple classes (Mh, Mr) were merged into one (termed Mh in this discussion as most were hard maple) due to almost complete overlap between signatures.

Table 4. Summary of Swan Lake species signature (Jeffries Matisuta Distance) separability analysis.

| | | | | | | | | | |
|---------------|---------------|---------------|---------------|---------------|---------------|---------------|---------------|-----------|------------|
| Mh | Be | By | He | Pw | Sw | Bf | Ce | | Avg |
| 0.0000 | 1.2544 | 1.7800 | 1.9994 | 1.9994 | 1.9997 | 2.0000 | 1.6842 | Mh | 1.8167 |
| 1.2544 | 0.0000 | 1.1242 | 1.7221 | 1.7945 | 1.8927 | 1.7955 | 1.1886 | Be | 1.5389 |
| 1.7800 | 1.1242 | 0.0000 | 1.0987 | 1.4538 | 1.1645 | 1.6081 | 0.9106 | By | 1.3057 |
| 1.9994 | 1.7221 | 1.0987 | 0.0000 | 0.9905 | 0.8393 | 0.9201 | 1.3762 | He | 1.2781 |
| 1.9994 | 1.7945 | 1.4538 | 0.9905 | 0.0000 | 0.9512 | 1.1729 | 1.4008 | Pw | 1.3947 |
| 1.9997 | 1.8927 | 1.1645 | 0.8393 | 0.9512 | 0.0000 | 1.5466 | 1.4155 | Sw | 1.4014 |
| 2.0000 | 1.7955 | 1.6081 | 0.9201 | 1.1729 | 1.5466 | 0.0000 | 1.4902 | Bf | 1.5048 |
| 1.6842 | 1.1886 | 0.9106 | 1.3762 | 1.4008 | 1.4155 | 1.4902 | 0.0000 | Ce | 1.3523 |

An examination of the species signature separability analysis of the final eight signatures (Table 4) reveals good separability between several species pairs (e.g. Bf-Mh, [2.0]; Sw-Mh, [1.9997]; Be-Pw, [1.7945]), but poor separability between others. In particular, there appears to be much spectral overlap between most softwood pairs; however, most softwood signatures showed relatively good separability from most hardwood signatures. It is expected; however, that relatively high spectral overlap between the signatures of some species will likely translate into confusion between those classes in the classification result.

Classification (and stand delineation) results for the Swan Lake validation tiles are presented in Figure 17 and Figure 18.

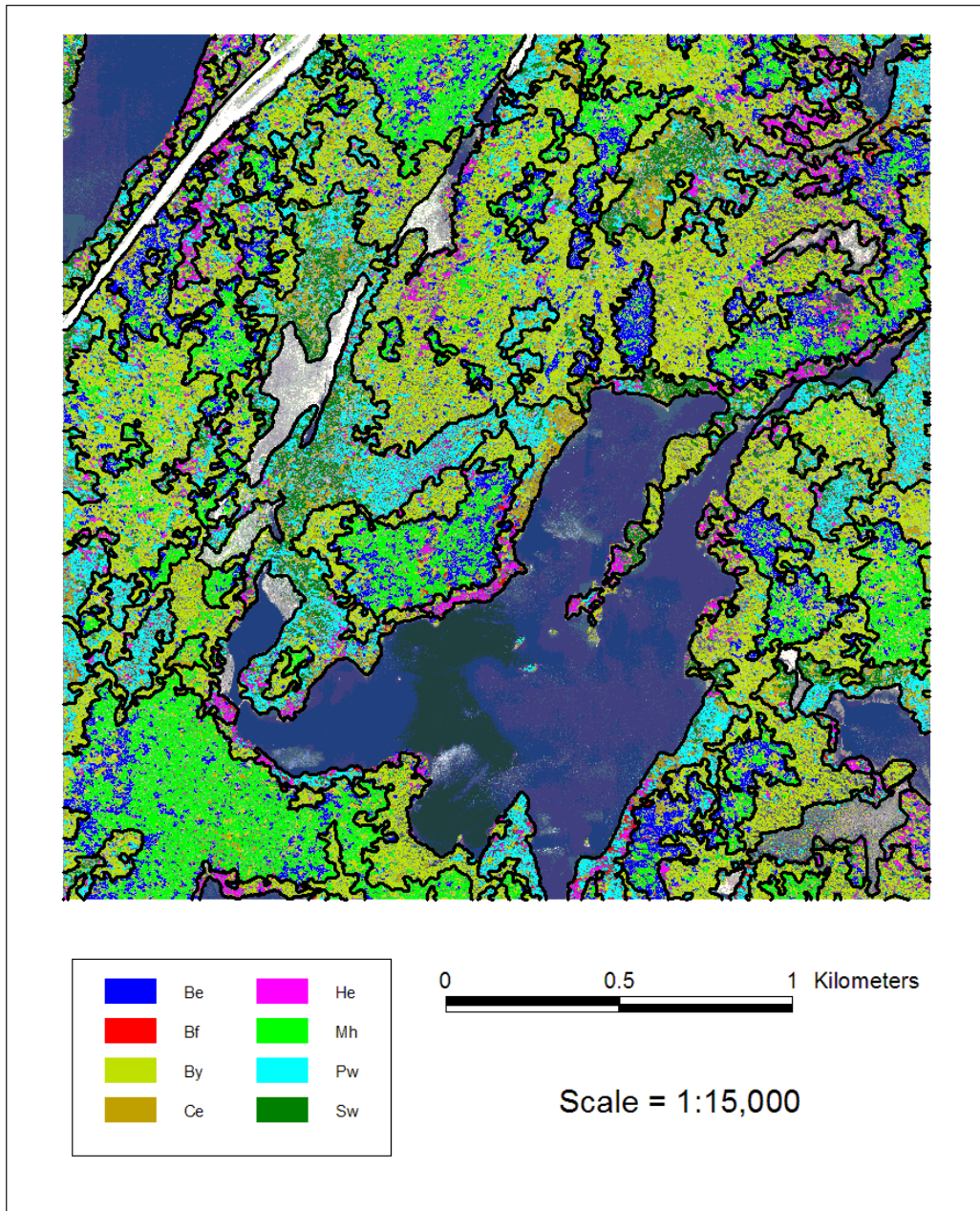


Figure 17. Classification and delineation result: Swan Lake (67504_A4).

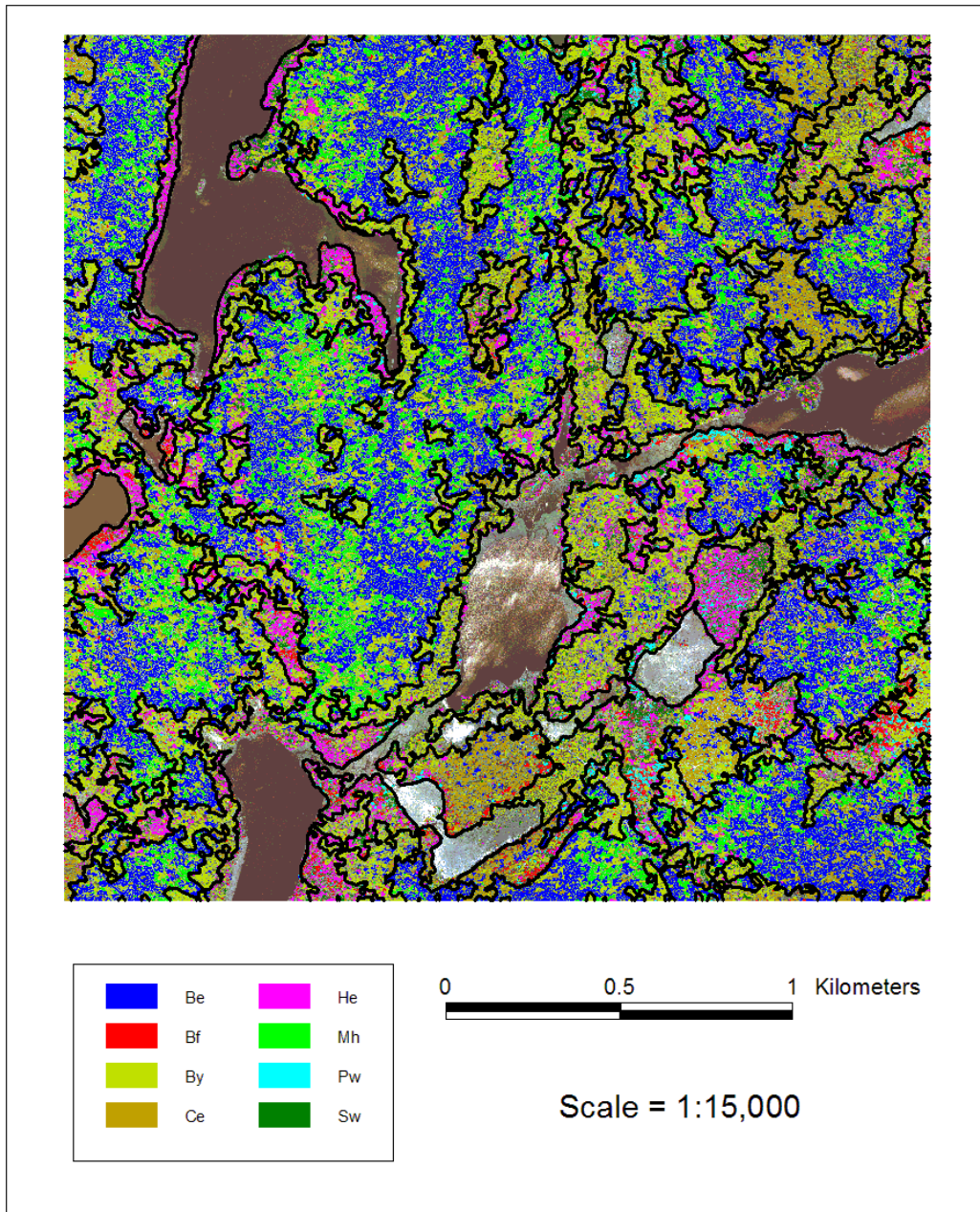


Figure 18. Classification and delineation result: Swan Lake (67503_D4).

6.3.2. *Petawawa Research Forest Species Signatures and Classification with Methods 1–3*

Training data for the Petawawa site were collected across 12 image tiles. The original Petawawa training data spanned 17 species, eventually resulting in 11 classes (Pt, Aw, Bd, Bf, Bw, Ce, Mh, Pr, Pw, Sb, Sw). Elimination or merging of classes was done after consultation with OMNR and with consideration to species separability analysis and sample size. A summary of species signature separability among the final 11 classes is presented in Table 5. Similar patterns of signature separability were observed in the Petawawa training data as is noted above for Swan Lake. The classification (and stand delineation) result for the Petawawa area is presented in Figure 19.

Table 5. Summary of species signature (Jeffries Matisuta Distance) separability analysis (Petawawa Research Forest).

| Pt | Aw | Bd | Bw | Mh | Bf | Ce | Pr | Pw | Sb | Sw | | Avg |
|---------------|---------------|---------------|---------------|---------------|---------------|---------------|---------------|---------------|---------------|---------------|-----------|--------|
| 0.0000 | 1.7866 | 1.9704 | 1.4497 | 1.7888 | 1.6283 | 1.8825 | 1.3135 | 1.6848 | 1.8927 | 1.9201 | Pt | 1.7317 |
| 1.7866 | 0.0000 | 1.5154 | 1.5047 | 1.7927 | 1.8780 | 1.9450 | 1.8647 | 1.8520 | 1.8463 | 1.9917 | Aw | 1.7977 |
| 1.9704 | 1.5154 | 0.0000 | 1.7255 | 1.4531 | 1.8440 | 1.7937 | 1.9264 | 1.6568 | 1.9553 | 1.8839 | Bd | 1.7724 |
| 1.4497 | 1.5047 | 1.7255 | 0.0000 | 1.4916 | 1.4643 | 1.8651 | 1.3878 | 1.3481 | 1.8531 | 1.9066 | Bw | 1.5996 |
| 1.7888 | 1.7927 | 1.4531 | 1.4916 | 0.0000 | 1.8042 | 1.8473 | 1.8180 | 0.9763 | 1.9319 | 1.9647 | Mh | 1.6869 |
| 1.6283 | 1.8780 | 1.8440 | 1.4643 | 1.8042 | 0.0000 | 1.7517 | 1.2461 | 1.2667 | 1.3096 | 1.4191 | Bf | 1.5612 |
| 1.8825 | 1.9450 | 1.7937 | 1.8651 | 1.8473 | 1.7517 | 0.0000 | 1.9150 | 1.7838 | 1.9149 | 1.6741 | Ce | 1.8373 |
| 1.3135 | 1.8647 | 1.9264 | 1.3878 | 1.8180 | 1.2461 | 1.9150 | 0.0000 | 1.2286 | 1.4327 | 1.4210 | Pr | 1.5554 |
| 1.6848 | 1.8520 | 1.6568 | 1.3481 | 0.9763 | 1.2667 | 1.7838 | 1.2286 | 0.0000 | 1.2458 | 1.6815 | Pw | 1.4724 |
| 1.8927 | 1.8463 | 1.9553 | 1.8531 | 1.9319 | 1.3096 | 1.9149 | 1.4327 | 1.2458 | 0.0000 | 1.0382 | Sb | 1.6420 |
| 1.9201 | 1.9917 | 1.8839 | 1.9066 | 1.6741 | 1.4191 | 1.6741 | 1.4210 | 1.6815 | 1.0382 | 0.0000 | Sw | 1.6901 |

6.3.3 *Petawawa Research Forest Classification with Method 4*

The fourth approach to signature generation and species classification called for the delineation of sizeable (50–200 trees) single species areas on the screen and then, their identification by the interpreter or, as a last resort, by a visit to the site. This approach, based on the ‘look’ of different species on the image, tends to separate not only species, but specific instances of species (young vs. mature, well illuminated vs. backlit, etc.) and thus, invariably leads to more than just a breakdown of interesting species into an equal number of classes. These additional signatures lead to additional classes that can be regrouped later (i.e., as post-processing) to present the final classification results and when summarizing the ITC analysis results by forest stand polygons.

One can display classification results and accuracy as a confusion matrix. The standard confusion matrix is done using independent test areas, similar, yet distinct, from the training areas. It portrays how many trees from an area said to be made of a single species were classified as members of that species and how many were classified as members of the other classes. The percentage of trees that were correctly classified (i.e., into that

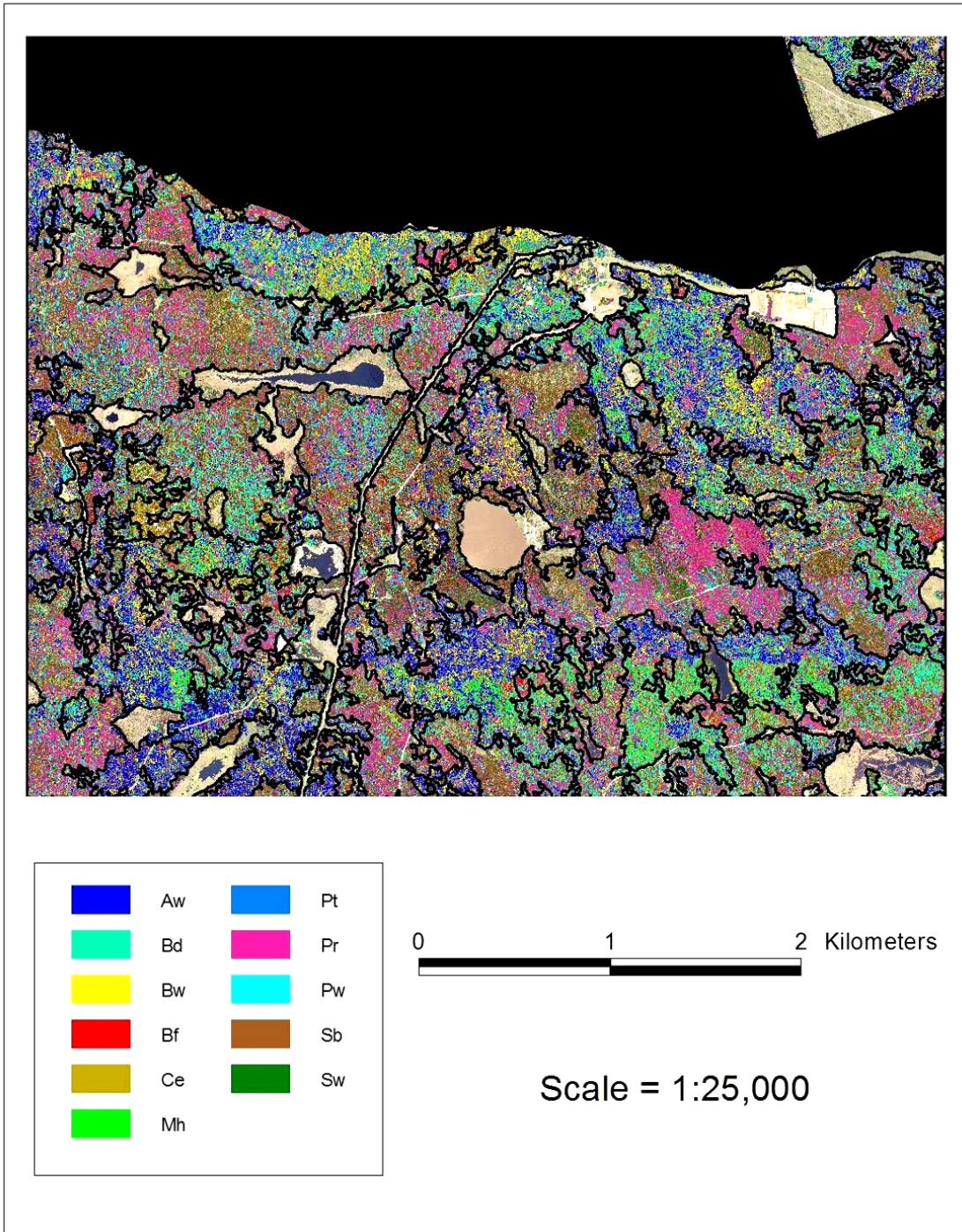


Figure 19. Classification and delineation result: Petawawa validation area.

same species or class) is said to be the classification accuracy of that class. To test the ‘robustness’ of a classification, two independent sets of testing areas could be used. Another traditional approach would be to exchange the role of the training or testing areas to see if consistent results are achieved. In our situation (i.e., a large mosaic of aerial data), selecting testing areas at a distant location from the training areas should also illustrate the strength of the intra and inter image normalization (done with the BRDF correction module).

However here, because of our obvious difficulties (see Appendix 1) in normalizing the radiances throughout the full PRF area, using independent and distant testing areas would only illustrate this weakness and would tell us very little about the intrinsic species separability capability of such aerial sensors. For this reason, the following confusion matrix (Table 6) was gathered using (as testing areas) the same areas that had been used to train the classifier. This inbred accuracy, becomes more a measure of species separability or species classification precision, than one of species classification accuracy.

Method 4 leads to an average species accuracy (or precision) of 67.6% (Table 6). However, if we recombine (as post-processing) the two poplar classes (Po young [Po y] and Po old [Po o]) and the two white pine classes (Pw young [Pw y] and Pw old [Pw o]), giving us an accuracy of 92.5% for the poplars and of 63.7% for the white pines, **we then get an average species accuracy (or precision, here) of around 76%, for the separation of 10 species.** Most species have reasonable accuracies (around 65–75%), except for soft maple (Ms) and jack pine (Pj). For jack pine, the issue was traced back to having multiple training areas, some of them from differently radiometrically balanced images. For soft maple (Ms), the majority of the confusion is with white birch (Bw), an understandable situation. Thus, Method 4 leads to good results with a minimum amount of efforts and minimal field work requirements. It is the more operation-oriented approach.

Table 6. Method 4 confusion matrix (testing areas=training areas) of twelve classes portraying ten species.

| | Mh | Ms | Or | Bw | Po y | Po o | Pw y | Pj | Pr | Sw | Sb | Pw o |
|------|-----------|----------|-----------|----------|-----------|----------|----------|-----------|-----------|-----------|-----------|-----------|
| Mh | 122 74.8% | 0 0.0% | 1 0.6% | 0 0.0% | 0 0.0% | 0 0.0% | 3 2.7% | 60 3.0% | 0 0.0% | 2 1.0% | 30 8.9% | 45 15.3% |
| Ms | 2 1.2% | 92 44.9% | 1 0.6% | 3 7.0% | 0 0.0% | 1 0.7% | 0 0.0% | 3 0.1% | 1 0.3% | 0 0.0% | 0 0.0% | 6 2.0% |
| Or | 0 0.0% | 1 0.5% | 121 67.2% | 0 0.0% | 0 0.0% | 5 3.4% | 0 0.0% | 2 0.1% | 22 7.1% | 1 0.5% | 0 0.0% | 2 0.7% |
| Bw | 1 0.6% | 73 35.6% | 0 0.0% | 38 88.4% | 0 0.0% | 3 2.0% | 0 0.0% | 0 0.0% | 1 0.3% | 0 0.0% | 0 0.0% | 0 0.0% |
| Po y | 0 0.0% | 1 0.5% | 2 1.1% | 0 0.0% | 106 89.1% | 37 25.2% | 0 0.0% | 0 0.0% | 0 0.0% | 0 0.0% | 0 0.0% | 0 0.0% |
| Po o | 2 1.2% | 2 1.0% | 17 9.4% | 0 0.0% | 9 7.6% | 94 63.9% | 0 0.0% | 0 0.0% | 3 1.0% | 0 0.0% | 0 0.0% | 0 0.0% |
| Pw y | 10 6.1% | 10 4.9% | 0 0.0% | 1 2.3% | 0 0.0% | 1 0.7% | 95 86.4% | 279 13.9% | 8 2.6% | 0 0.0% | 0 0.0% | 25 8.5% |
| Pj | 2 1.2% | 1 0.5% | 0 0.0% | 0 0.0% | 0 0.0% | 0 0.0% | 0 0.0% | 446 22.2% | 1 0.3% | 11 5.6% | 19 5.6% | 22 7.5% |
| Pr | 0 0.0% | 8 3.9% | 31 17.2% | 0 0.0% | 0 0.0% | 2 1.4% | 5 4.5% | 189 9.4% | 244 79.2% | 17 8.7% | 0 0.0% | 38 12.9% |
| Sw | 5 3.1% | 1 0.5% | 2 1.1% | 0 0.0% | 0 0.0% | 0 0.0% | 0 0.0% | 466 23.2% | 5 1.6% | 141 72.3% | 8 2.4% | 9 3.1% |
| Sb | 4 2.5% | 0 0.0% | 0 0.0% | 0 0.0% | 0 0.0% | 0 0.0% | 0 0.0% | 322 16.1% | 0 0.0% | 6 3.1% | 261 77.4% | 1 0.3% |
| Pw o | 11 6.7% | 3 1.5% | 0 0.0% | 0 0.0% | 0 0.0% | 1 0.7% | 5 4.5% | 198 9.9% | 21 6.8% | 9 4.6% | 0 0.0% | 133 45.1% |
| Un | 4 2.5% | 13 6.3% | 5 2.8% | 1 2.3% | 4 3.4% | 3 2.0% | 2 1.8% | 40 2.0% | 2 0.6% | 8 4.1% | 19 5.6% | 14 4.7% |

XX XX.X% = number of crowns and percentage classified
 Un = Unclassified

6.3.4 Petawawa Research Forest Classification with Method 5

Because of our lack of success in normalizing radiances throughout even a selected sub-area (7 km x 8 km) of the Petawawa Research Forest (see Figure 11), the results of the fifth approach to signature generation and species classification (based on the combination of ITCs from training areas with individually delineated tree crowns and making use of outliers removal in the signature generation process) will also be judged using its inbred confusion matrix (testing areas = training areas). Table 7 shows the confusion between the main sixteen classes. **It led to an average accuracy (here, separation precision) of 53.7% and an overall accuracy of 65%, which is rather good for sixteen classes.**

There is some confusion between the three white pine classes (Pw i¹, Pw o², Pw b³) and the Larch class (La); more so for the 'bright' white pine. The 'immature' white pine also gets confused with the red pine and black spruce classes. There is also confusion between the hard maple class and the bright white pine class and, between the soft maple class and the aspens. The aspen classes (At, At pq⁴, and Alt) are mainly confused with each other and, to some extent, with other hardwood classes such as white birch and soft maple. White birch gets essentially classified as damaged white birch and, that later class appears mostly irrelevant, which we may have deducted by looking at Figure 9. The yellow birch class appears highly unstable, which is easily explained by the fact that it was based and is being tested with only eight (8) individuals. The classification of larch, red pine, white spruce, black spruce and jack pine is good, with some minor confusion among the coniferous trees.

Removing the two most irrelevant and unstable classes, damaged White Birch and Yellow Birch, led to a classification for which a confusion table is presented in Table 8. (**Note:** A few other classes had been removed even earlier (beech, basswood, balsam fir) for similar reasons and because the classification accuracy program (*ITCCA*) can only deal with a maximum of 16 classes). **This led to an average accuracy (here, separation precision) of 65.8% and an overall accuracy of 67.1%, for fourteen (14) classes.**

When the 14 classes are regrouped into the 10 species they represent, **an average accuracy (here, separation precision) of 74% and an overall accuracy (precision) of 70.4% are achieved** (Table 9). There is still some minor confusion amongst the coniferous species and amongst the deciduous species, the most important for the later resulting in a third of the soft maples being considered aspens. As usual, the white pine species, so easily pickup by shape by even casual photo interpreters, is a bit problematic as 26% of hard maple get classified as such and, significant quantities of white pines (15% and 11%) get classified as larches and red pines, respectively.

This illustrates the species separation potential of this sensor's 8 bit data (here, Vexcel Ultracam) and possibly, its classification potential given sufficiently well radiometrically-corrected images.

¹ Pw i = white pine immature

² Pw o – white pine old

³ Pw b = white pine bright

⁴ At pq = trembling aspen poor-quality

Table 7. The confusion matrix of the 16 classes (testing areas=training areas) from the ‘purified’ signatures obtained with Method 5.

| | Pw i | Pw o | Pw b | Mh | Ms | Bw d | Bw | At | At pq | Alt | By | La | Pr | Sw | Sb | Pj |
|-------|----------|-----------|----------|-----------|----------|----------|----------|----------|----------|----------|---------|---------|-----------|-----------|-----------|----------|
| Pw i | 80 33.3% | 7 3.6% | 4 7.5% | 3 1.6% | 0 0.0% | 2 5.7% | 0 0.0% | 0 0.0% | 0 0.0% | 0 0.0% | 2 25.0% | 3 1.4% | 20 3.7% | 0 0.0% | 4 0.7% | 0 0.0% |
| Pw o | 14 5.8% | 101 51.5% | 1 1.9% | 15 8.2% | 0 0.0% | 1 2.9% | 0 0.0% | 0 0.0% | 0 0.0% | 0 0.0% | 1 12.5% | 11 5.1% | 26 4.8% | 2 0.5% | 1 0.2% | 2 2.2% |
| Pw b | 12 5.0% | 12 6.1% | 30 56.6% | 28 15.3% | 0 0.0% | 0 0.0% | 0 0.0% | 0 0.0% | 0 0.0% | 0 0.0% | 0 0.0% | 13 6.0% | 0 0.0% | 0 0.0% | 16 2.9% | 0 0.0% |
| Mh | 1 0.4% | 11 5.6% | 2 3.8% | 121 66.1% | 0 0.0% | 0 0.0% | 0 0.0% | 0 0.0% | 0 0.0% | 0 0.0% | 1 12.5% | 1 0.5% | 0 0.0% | 2 0.5% | 1 0.2% | 0 0.0% |
| Ms | 9 3.8% | 1 0.5% | 0 0.0% | 0 0.0% | 12 66.7% | 0 0.0% | 0 0.0% | 7 10.9% | 3 8.6% | 1 5.0% | 0 0.0% | 0 0.0% | 51 9.4% | 0 0.0% | 0 0.0% | 0 0.0% |
| Bw d | 0 0.0% | 0 0.0% | 0 0.0% | 0 0.0% | 0 0.0% | 3 8.6% | 28 90.3% | 2 3.1% | 0 0.0% | 0 0.0% | 0 0.0% | 0 0.0% | 0 0.0% | 0 0.0% | 0 0.0% | 0 0.0% |
| Bw | 0 0.0% | 0 0.0% | 0 0.0% | 0 0.0% | 0 0.0% | 0 0.0% | 1 3.2% | 8 12.5% | 0 0.0% | 1 5.0% | 0 0.0% | 0 0.0% | 1 0.2% | 0 0.0% | 0 0.0% | 0 0.0% |
| At | 0 0.0% | 0 0.0% | 0 0.0% | 0 0.0% | 3 16.7% | 0 0.0% | 1 3.2% | 17 26.6% | 1 2.9% | 0 0.0% | 0 0.0% | 0 0.0% | 6 1.1% | 0 0.0% | 0 0.0% | 0 0.0% |
| At pq | 7 2.9% | 0 0.0% | 0 0.0% | 0 0.0% | 1 5.6% | 0 0.0% | 0 0.0% | 3 4.7% | 20 57.1% | 0 0.0% | 0 0.0% | 8 3.7% | 9 1.7% | 0 0.0% | 0 0.0% | 0 0.0% |
| Alt | 5 2.1% | 3 1.5% | 0 0.0% | 1 0.5% | 2 11.1% | 0 0.0% | 0 0.0% | 24 37.5% | 8 22.9% | 17 85.0% | 0 0.0% | 4 1.8% | 18 3.3% | 0 0.0% | 0 0.0% | 0 0.0% |
| By | 4 1.7% | 5 2.6% | 0 0.0% | 2 1.1% | 0 0.0% | 9 25.7% | 1 3.2% | 0 0.0% | 0 0.0% | 0 0.0% | 2 25.0% | 0 0.0% | 5 0.9% | 1 0.3% | 0 0.0% | 0 0.0% |
| La | 30 12.5% | 28 14.3% | 14 26.4% | 7 3.8% | 0 0.0% | 0 0.0% | 0 0.0% | 0 0.0% | 0 0.0% | 0 0.0% | 0 0.0% | 0 0.0% | 159 73.3% | 3 0.6% | 0 0.0% | 7 1.3% |
| Pr | 40 16.7% | 14 7.1% | 0 0.0% | 1 0.5% | 0 0.0% | 0 0.0% | 0 0.0% | 3 4.7% | 1 2.9% | 1 5.0% | 2 25.0% | 9 4.1% | 369 68.2% | 8 2.1% | 0 0.0% | 4 4.3% |
| Sw | 0 0.0% | 2 1.0% | 0 0.0% | 0 0.0% | 0 0.0% | 0 0.0% | 0 0.0% | 0 0.0% | 0 0.0% | 0 0.0% | 0 0.0% | 0 0.0% | 5 0.9% | 261 67.8% | 29 5.3% | 2 2.2% |
| Sb | 29 12.1% | 2 1.0% | 2 3.8% | 0 0.0% | 0 0.0% | 0 0.0% | 0 0.0% | 0 0.0% | 0 0.0% | 0 0.0% | 0 0.0% | 1 0.5% | 0 0.0% | 42 10.9% | 461 84.0% | 1 1.1% |
| Pj | 6 2.5% | 6 3.1% | 0 0.0% | 0 0.0% | 0 0.0% | 0 0.0% | 0 0.0% | 0 0.0% | 0 0.0% | 0 0.0% | 0 0.0% | 2 0.9% | 19 3.5% | 58 15.1% | 12 2.2% | 80 87.0% |
| Un | 3 1.3% | 4 2.0% | 0 0.0% | 5 2.7% | 0 0.0% | 20 57.1% | 0 0.0% | 0 0.0% | 2 5.7% | 0 0.0% | 0 0.0% | 6 2.8% | 9 1.7% | 11 2.9% | 18 3.3% | 3 3.3% |

XX XX.X% = number of crowns and percentage classified
 Un = Unclassified

Table 8. The confusion matrix (testing areas=training areas) for a 14 class classification with Method 5 (dropping two classes).

| | Pw i | Pw o | Pw b | Mh | Ms | Bw | At | Atpq | Alt | La | Pr | Sw | Sb | Pj |
|------|----------|-----------|----------|-----------|----------|----------|----------|----------|----------|-----------|-----------|-----------|-----------|----------|
| Pw i | 81 33.8% | 7 3.6% | 4 7.5% | 4 2.2% | 0 0.0% | 0 0.0% | 0 0.0% | 0 0.0% | 0 0.0% | 3 1.4% | 22 4.1% | 0 0.0% | 4 0.7% | 0 0.0% |
| Pw o | 14 5.8% | 104 53.1% | 1 1.9% | 16 8.7% | 0 0.0% | 0 0.0% | 0 0.0% | 0 0.0% | 0 0.0% | 11 5.1% | 26 4.8% | 3 0.8% | 1 0.2% | 2 2.2% |
| Pw b | 12 5.0% | 12 6.1% | 30 56.6% | 28 15.3% | 0 0.0% | 0 0.0% | 0 0.0% | 0 0.0% | 0 0.0% | 13 6.0% | 0 0.0% | 0 0.0% | 16 2.9% | 0 0.0% |
| Mh | 1 0.4% | 11 5.6% | 2 3.8% | 121 66.1% | 0 0.0% | 0 0.0% | 0 0.0% | 0 0.0% | 0 0.0% | 1 0.5% | 0 0.0% | 2 0.5% | 1 0.2% | 0 0.0% |
| Ms | 11 4.6% | 2 1.0% | 0 0.0% | 0 0.0% | 12 66.7% | 0 0.0% | 7 10.9% | 3 8.6% | 1 5.0% | 0 0.0% | 52 9.6% | 0 0.0% | 0 0.0% | 0 0.0% |
| Bw | 0 0.0% | 0 0.0% | 0 0.0% | 0 0.0% | 0 0.0% | 30 96.8% | 10 15.6% | 0 0.0% | 1 5.0% | 0 0.0% | 1 0.2% | 0 0.0% | 0 0.0% | 0 0.0% |
| At | 0 0.0% | 0 0.0% | 0 0.0% | 0 0.0% | 3 16.7% | 1 3.2% | 17 26.6% | 1 2.9% | 0 0.0% | 0 0.0% | 6 1.1% | 0 0.0% | 0 0.0% | 0 0.0% |
| Atpq | 7 2.9% | 0 0.0% | 0 0.0% | 0 0.0% | 1 5.6% | 0 0.0% | 3 4.7% | 20 57.1% | 0 0.0% | 8 3.7% | 9 1.7% | 0 0.0% | 0 0.0% | 0 0.0% |
| Alt | 5 2.1% | 4 2.0% | 0 0.0% | 1 0.5% | 2 11.1% | 0 0.0% | 24 37.5% | 8 22.9% | 17 85.0% | 4 1.8% | 20 3.7% | 0 0.0% | 0 0.0% | 0 0.0% |
| La | 30 12.5% | 28 14.3% | 14 26.4% | 7 3.8% | 0 0.0% | 0 0.0% | 0 0.0% | 0 0.0% | 0 0.0% | 159 73.3% | 3 0.6% | 0 0.0% | 7 1.3% | 0 0.0% |
| Pr | 41 17.1% | 14 7.1% | 0 0.0% | 1 0.5% | 0 0.0% | 0 0.0% | 3 4.7% | 1 2.9% | 1 5.0% | 9 4.1% | 369 68.2% | 8 2.1% | 0 0.0% | 4 4.3% |
| Sw | 0 0.0% | 2 1.0% | 0 0.0% | 0 0.0% | 0 0.0% | 0 0.0% | 0 0.0% | 0 0.0% | 0 0.0% | 0 0.0% | 5 0.9% | 261 67.8% | 29 5.3% | 2 2.2% |
| Sb | 29 12.1% | 2 1.0% | 2 3.8% | 0 0.0% | 0 0.0% | 0 0.0% | 0 0.0% | 0 0.0% | 0 0.0% | 1 0.5% | 0 0.0% | 42 10.9% | 461 84.0% | 1 1.1% |
| Pj | 6 2.5% | 6 3.1% | 0 0.0% | 0 0.0% | 0 0.0% | 0 0.0% | 0 0.0% | 0 0.0% | 0 0.0% | 2 0.9% | 19 3.5% | 58 15.1% | 12 2.2% | 80 87.0% |
| Un | 3 1.3% | 4 2.0% | 0 0.0% | 5 2.7% | 0 0.0% | 0 0.0% | 0 0.0% | 2 5.7% | 0 0.0% | 6 2.8% | 9 1.7% | 11 2.9% | 18 3.3% | 3 3.3% |

XX XX.X% = number of crowns and percentage classified

Un = Unclassified

Table 9. The confusion matrix (in %) for the 14 classes in Method 5 when regrouped into the 10 species they represent.

| | Pw | Mh | Ms | Bw | As | La | Pr | Sw | Sb | Pj |
|--------|--------------|--------------|--------------|--------------|--------------|--------------|--------------|--------------|--------------|--------------|
| Pw | 54.19 | 26.23 | 0.00 | 0.00 | 0.00 | 12.44 | 8.87 | 0.78 | 3.83 | 2.17 |
| Mh | 2.86 | 66.12 | 0.00 | 0.00 | 0.00 | 0.46 | 0.00 | 0.52 | 0.18 | 0.00 |
| Ms | 2.66 | 0.00 | 66.67 | 0.00 | 9.24 | 0.00 | 9.61 | 0.00 | 0.00 | 0.00 |
| Bw | 0.00 | 0.00 | 0.00 | 96.77 | 9.24 | 0.00 | 0.18 | 0.00 | 0.00 | 0.00 |
| As | 3.27 | 0.55 | 33.33 | 3.23 | 75.63 | 5.53 | 6.47 | 0.00 | 0.00 | 0.00 |
| La | 14.72 | 3.83 | 0.00 | 0.00 | 0.00 | 73.27 | 0.55 | 0.00 | 1.28 | 0.00 |
| Pr | 11.25 | 0.55 | 0.00 | 0.00 | 4.20 | 4.15 | 68.21 | 2.08 | 0.00 | 4.35 |
| Sw | 0.41 | 0.00 | 0.00 | 0.00 | 0.00 | 0.00 | 0.92 | 67.79 | 5.28 | 2.17 |
| Sb | 6.75 | 0.00 | 0.00 | 0.00 | 0.00 | 0.46 | 0.00 | 10.91 | 83.97 | 1.09 |
| Pj | 2.45 | 0.00 | 0.00 | 0.00 | 0.00 | 0.92 | 3.51 | 15.06 | 2.19 | 86.96 |
| Un | 1.43 | 2.73 | 0.00 | 0.00 | 1.68 | 2.76 | 1.66 | 2.86 | 3.28 | 3.26 |
| # ITCs | 489 | 183 | 18 | 31 | 119 | 217 | 541 | 385 | 549 | 92 |

As = All Aspens

Un = Unclassified

ITCs = number of segmented crowns being evaluated

At this point, very little can be said about the potential of the 12-14 bit data typically produced by the sensor.

6.4. Forest Stand Polygon Delineation

Output from the automated forest stand polygon delineation process was reviewed and edited by a Silvatech interpreter. Final delineation results are shown in Figures 20, 21 & 22. Overall, the polygon delineation results were assessed as a good start for further segmentation of smaller stands within some of the larger polygons. Although not perfect, the line work produced through the automated process is consistent across image tiles and provides a good starting point for interpreters. If applied operationally, the delineation would increase the efficiency of interpreters and lead to a more consistent and possibly more precise delineation product than one produced solely through manual means.

For the Swan Lake site, polygons required minor edge matching in a few cases where there was an offset between polygons along the boundary of the two validation tiles (a function of deriving automated polygons by tile). In two cases small polygons were deleted where they started on one tile but did not continue on the adjacent tile. Overall, major timber types were well-delineated, although the output was viewed as inconsistent in some areas, especially in consideration of height and density differences.

The Petawawa output did not require edge matching since the validation tiles were mosaicked prior to analysis. The automated polygons were all complete and were left 'as is' without manual alteration. Delineation based on changes in timber type was good, as was distinction of non-treed areas, swamps, and wetlands.

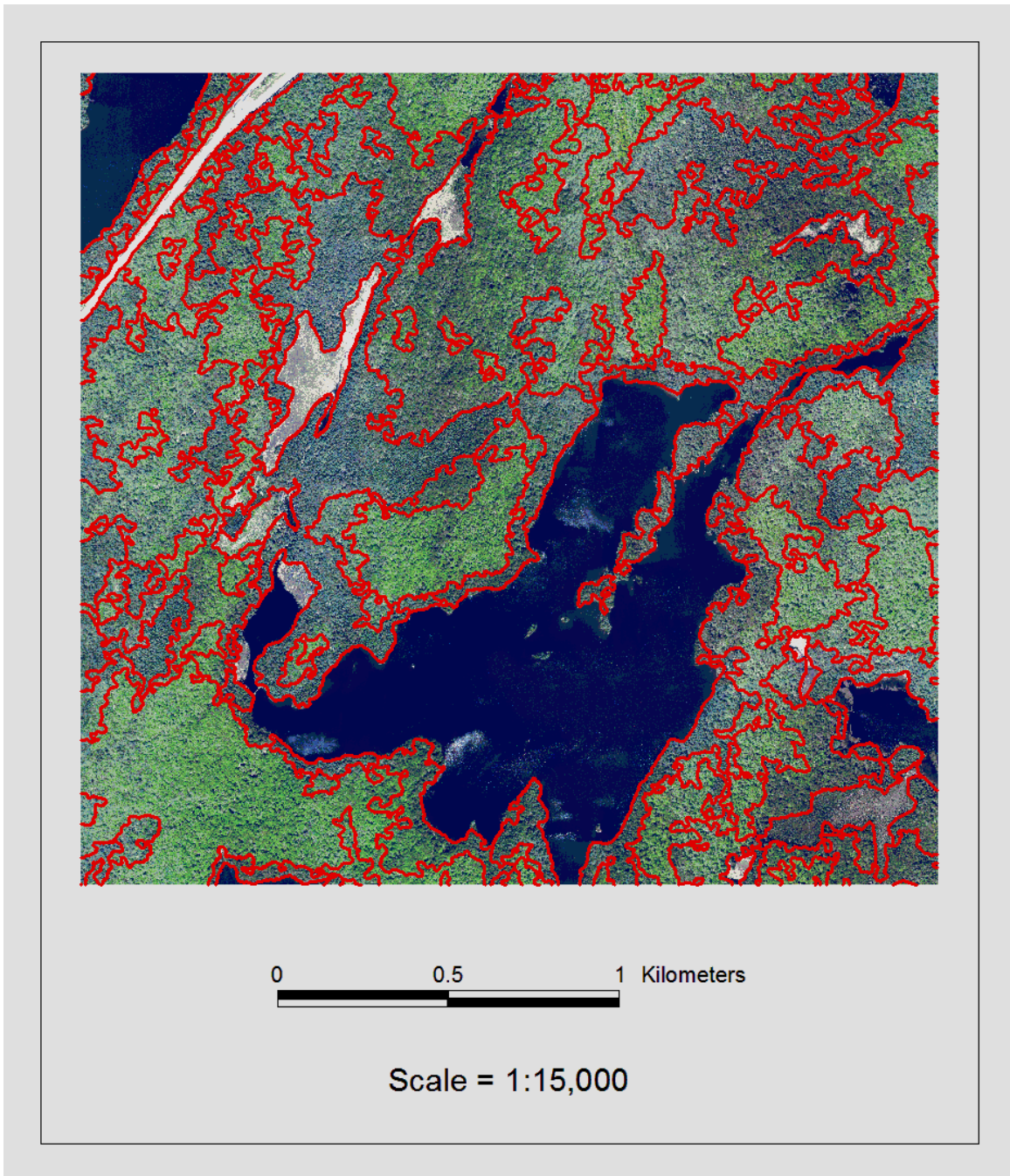


Figure 20. Delineation result: Swan Lake (67504_A4).

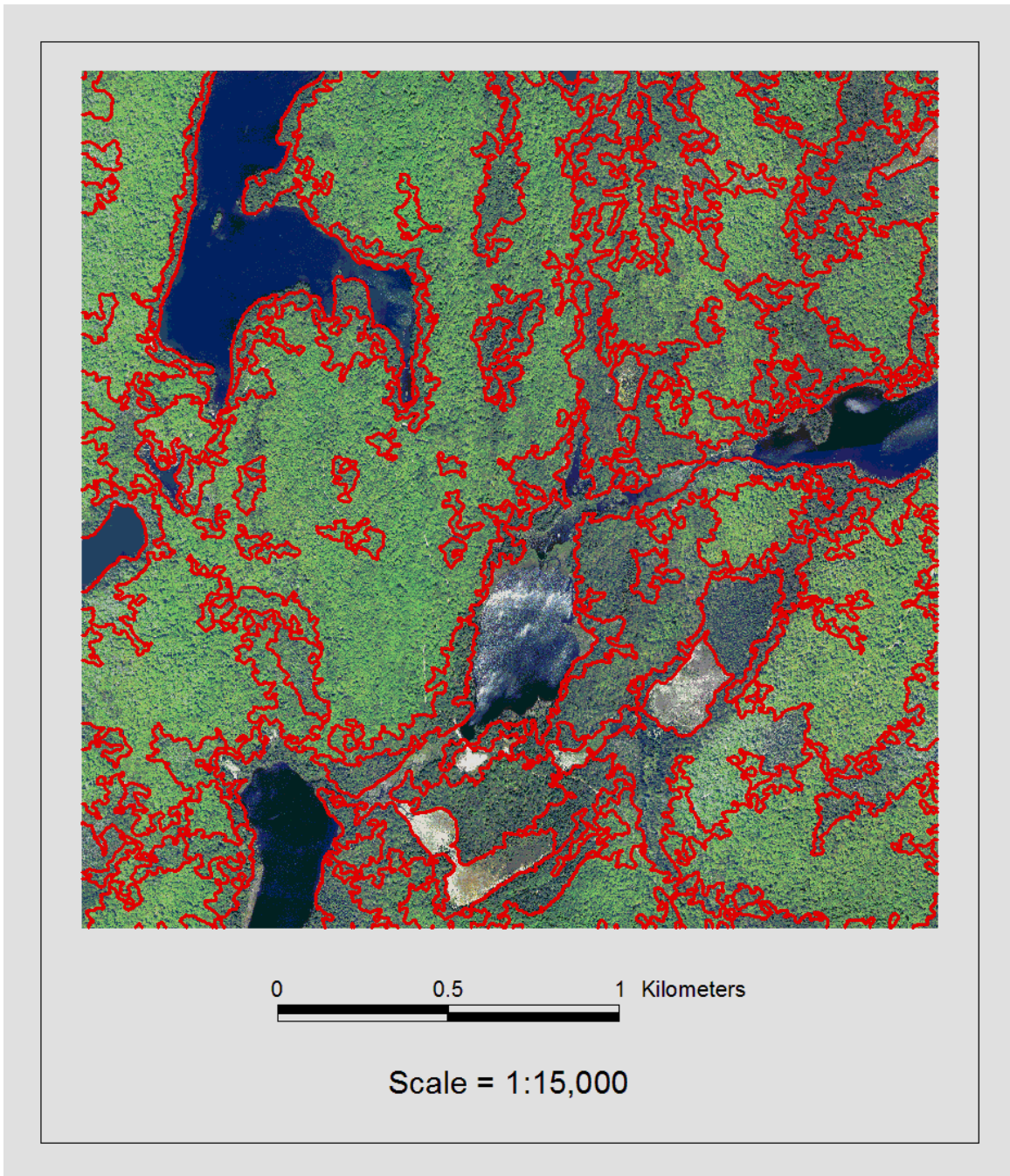


Figure 21. Delineation result: Swan Lake (67503_D4).

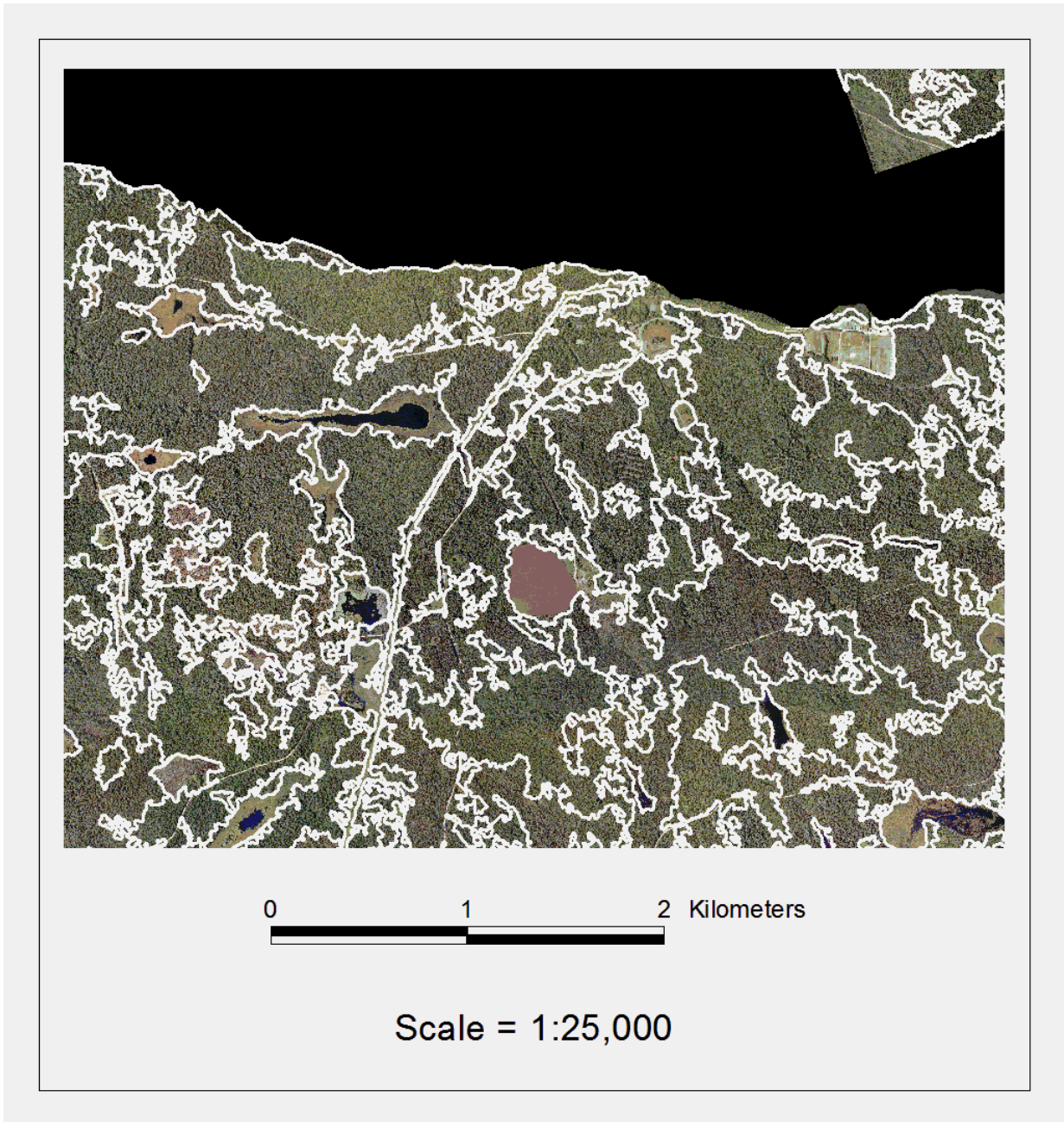


Figure 22. Delineation result: Petawawa validation area.

6.5. The Role of LiDAR

Although the main focus of this project was to extract forest resource information from digital *imagery*, the importance of *LiDAR* within that process should not be overlooked. While the performance of the *ITC Suite* tools is remarkable in its ability to identify and delineate trees, mechanisms are needed to constrain the ITC algorithms to the forest canopy or differentiate trees from other features in the species classification process.

A mask of non-forest area was created by specifying image threshold parameters using the *ITC Suite* pre-processing tools themselves. However, areas of vegetated non-forest were not successfully masked out and a few areas of forest canopy were inadvertently masked. These resulted in either commission or omission errors in the tree isolation depending on threshold settings. Due to the high spectral variability characteristics of high spatial resolution digital imagery, it is difficult to isolate all areas of interest (i.e. valid forest areas) based solely on spectral values due to significant spectral overlap between the forest canopy and other areas with similar spectral properties (such as vegetated forest gaps, meadows, clearings, etc.).

A comparison of image-only (spectral-based) masking versus LiDAR-based masking is presented in Figure 23. The extent to which non-forest areas could be distinguished from valid forest canopy (a) based solely on spectral thresholds from the imagery was very limited, resulting in an incomplete non-forest mask (b). Large tracts of non-forest areas could not be included in the spectral-based mask without also masking out valid forest areas (due to spectral overlap between pixels within these non-forest areas and pixels within the valid forest canopy). Figure 23(c) shows the result of the LiDAR-based mask for the same area. Here, nearly all non-forest areas have been successfully masked while preserving valid forest areas.

Integration of LiDAR-derived surface models with image-derived spectral information produced an accurate stratification of forest vs. non-forest areas. Without the LiDAR data, creating a non-forest mask would have been much more difficult and less effective. The effect of using LiDAR-based masking to constrain ITC analysis to valid forest areas is illustrated in Figure 24. Here, non-forest areas such as clearings and gaps (a) are excluded from analysis using a LiDAR-based mask (b). The ITC tree crown delineation algorithm is constrained to areas of valid forest canopy only (c).

Additional benefits of LiDAR for forest inventory mensuration include the derivation of canopy height models and the calculation of tree-height-related attributes (e.g. stand height, stand height frequency distribution, stand basal area, stand volume) and quantification of non-productive land within timber license areas.

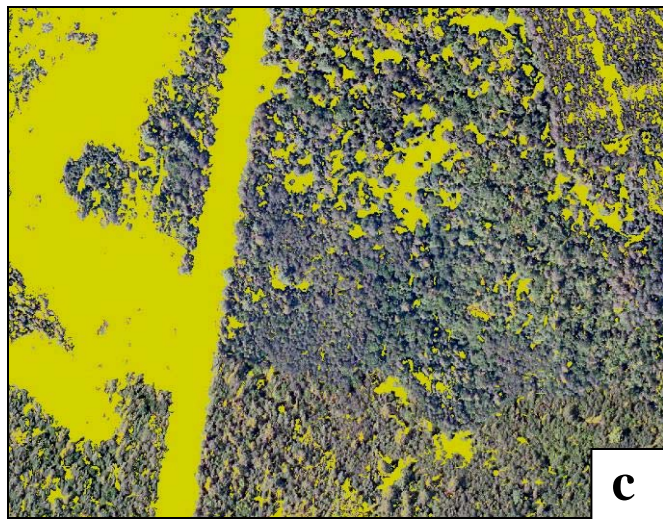
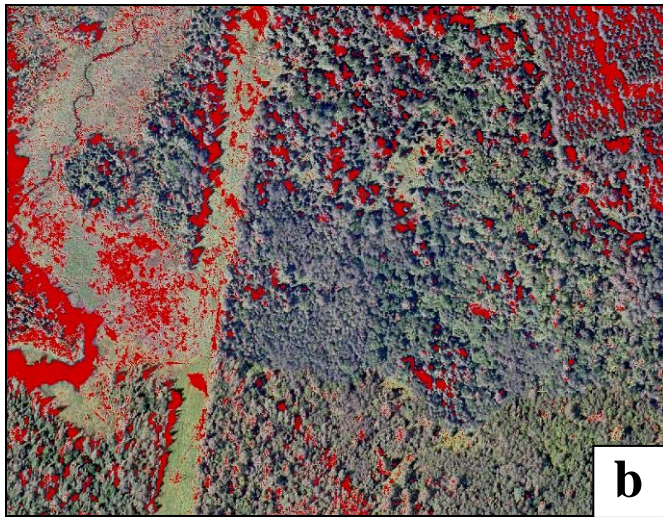


Figure 23. Comparison of spectral-based masking (b) versus LiDAR-based masking (c).

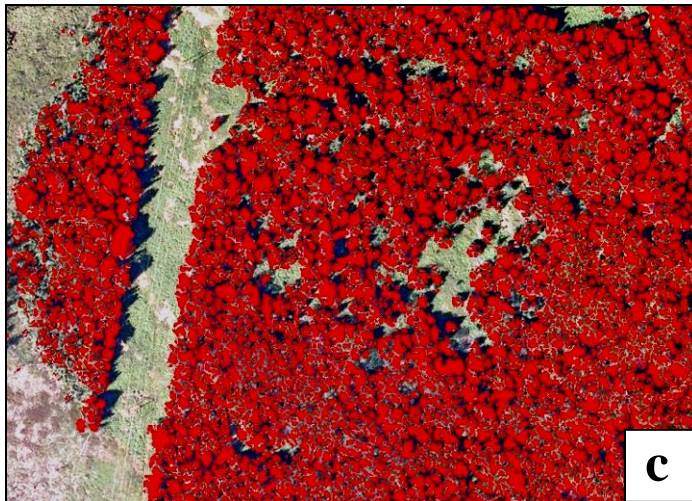


Figure 24. Non-forest areas such as clearings and forest gaps (a) are excluded from analysis using a LiDAR-based mask (b); subsequent ITC analysis is constrained to valid forest areas (c).

7. Challenges and Associated Consequences

7.1. Imagery Issues

Several unanticipated challenges arose during this project and are outlined here along with their impacts on overall project success. The most serious of these were imagery related.

Image spectral consistency was a problem in the data sets for both project sites. Image artefacts in the form of visible seam lines within orthophoto tiles, within-tile inconsistencies in view angle and spectral values, and significant differences in colour balancing between image tiles were present in both data sets (see Appendix 1). The image spectral consistency issue was partially addressed through a BRDF correction process as outlined in the Methods section and Appendix 1. While visible improvement to the overall consistency of both sets of imagery was evident, the results of the process in terms of image normalization were still far from optimal. This issue has had a major negative impact on classification accuracy as species signatures, derived from a limited number of training sites, are likely not representative of the spectral response of those species at all locations within the imagery.

The suggestion that a BRDF correction process be applied to original imagery *prior* to orthomosaicking is a key recommendation from this project and would likely lead to improved species classification results in future projects. In addition, one should avoid undocumented manual patching such as those done with the Vexcel UltraCam data set in an effort to remove clouds and cloud shadows from the mosaic.

7.2. Date of Image Acquisition (Leaf Status)

Timing of image acquisition compounded the spectral consistency issues for Swan Lake as the imagery were acquired in late spring before the deciduous canopy had reached full leaf-on status. Thus spectrally the hardwood tree spectral signatures were influenced strongly by the status of leaf flush and it was difficult to conduct and make conclusions regarding species classification. One of the theoretical advantages of aerial image acquisition over satellite imagery is the possibility to better control (by contract) the window of acquisition (time of the year, time of the day, meteorological conditions, etc.). It is critical to specify and enforce appropriate acquisition windows to obtain best results.

7.3. Implementation Hurdles

Although the *ITC Suite* has been used in the past to analyse aerial sensor data, this was the first time with such a sizeable dataset and with relatively unknown and unknowable sensors. As such, there was a lack of available information and expertise even from the

sensor operators and manufacturers regarding such things as specifications of the M7VI sensor, the nine panchromatic sections equalization process with the Vexcel Ultracam sensor, or the mosaicking process used by the data suppliers (see Appendix 1).

Other first time issues are listed below:

- First time with a dataset already georeferenced and mosaicked, and in some cases, manually retouched and colour-balanced. Although many modifications were made to the BRDF program to try desperately to compensate for such situations, it was ultimately to no avail.
- First time pushing the limits of the Windows XP (32 bit version) operating system (i.e., previous work had been done on Sun Solaris platforms, a superior but expensive environment). Under Windows, the size of the image disk files was not an issue as long as the NTFS filing system was used (older FAT32 disks are limited to 4GB). The limit for applications (programs) and applications accessible memory to store internally image channels for processing has been pushed to 3GB, the ultimate limit of user-accessible memory on the Windows XP (32 bit version) operating system.
- First time doing the ITC analyses in a more production oriented environment via the creation of multiple script files (EASI command files) to automate the process as much as possible working on multiple image tiles rather than a single huge image file.
- First time dealing with these particular ‘aerial image suppliers’, which meant also some first time issues for them. For example, First Base Solutions had just acquired the Vexcel UltraCam sensor system and were not at a full understanding of all of its features, nor on the proper processing software to use. Both First Base Solutions and M7VI struggled with the concept that digital image analysis needs are different from those of just plain visual assessments or even image interpretation. There were also technical issues that needed to be explained such as how to provide data in more than 8 bit resolution.
- First time for the Silvatech image analyst with the *ITC Suite*, thus lots of training needed lots of trials and errors, and implementation misunderstandings. On the other hand, good insight was provided from their perspective on procedures and improvements to be made to the process.
- First time for a group of this size, with a variety of responsibilities and working together from different end of the country, to carry out such a demanding project; it worked well and did not have detrimental effects on the project.
- First time with soft-copy interpretation software (i.e., PurView™) and the non-availability of proper models for these sensors.

8. Summary of Achievements

This project resulted in many achievements on a variety of aspects of semi-automated forest inventory production. One such achievement was the enhancement of the abilities of the entire *ITC Suite* software package to ingest and process large quantities of aerial digital imagery. The cooperation between Silvatech and the CFS in identifying and resolving these software-related issues has resulted in a more robust suite of software, presently running under PCI Geomatica v9x on Windows XP-32 platforms. Of course, these enhancements will be carried to other versions of PCI and other platforms in the future.

A better understanding of the field data requirements to support various automated image analysis approaches has also been gained through this project. For speciation, rather than focus the data collection on individual trees of target species, it is more efficient to locate on the image sizeable areas populated by a single species (30–200 crowns), with cursory verifications in the field of these species identities (i.e., Method 4). The number of samples and classes required to adequately represent any given species will likely vary by species and range of appearance across different environmental conditions and can also be affected by the timing and quality of the imagery. As with the conventional inventory process, individual tree and/or plot-based information will still be needed to establish local volume regression equations.

Until an automatic (or semi-automatic) version of Method 5, that allows for the removal of outliers from the signature generation process is implemented, Method 4 has to be the recommended approach, especially in an operational setting, as it leads to good results with a minimum amount of effort. It essentially relies on the interpreter's skills, with some cursory field visits to supplement or verify his/her assertions. It should be the most efficient, quickest, and most economical approach.

During the course of this project (and a previous one concentrating on Ontario's boreal forests) invaluable information was gathered (and sometimes, reversed engineered) on the details and hidden specifications of some of the newest airborne sensors, the different imagery needs of digital image analysis and soft-copy image interpretation, the needed complexity (and sometimes impossibility) of within image BRDF corrections and between images normalization (see Appendix 1).

The most significant achievement is the demonstration that semi-automated individual tree crown segmentation and classification algorithms and, the subsequent methodology for regrouping crowns into forest stands and reporting tree level attributes, have a very high potential to produce meaningful results when using 'proper' digital aerial multispectral imagery, especially when supported by LiDAR-based canopy height models. In addition, we have demonstrated that the ITC software can be used in an operational setting within a reasonable amount of time and should be able to deliver estimation of inventory attributes at the stand level while increasing the objectivity of the

resultant inventory. The day when image and LiDAR sensor data is loaded into a computer and a complete forest inventory is produced with one push of a button is an ideal goal and still in our future. However, the results of this project and the operational methods we continue to learn and incorporate along the way, are effective and viable tools that can be used today in the development of resource inventories. The tangible incremental products, techniques and methods developed to date, demonstrate that further development of such techniques and work towards the ultimate goal of a fully automated method is worth pursuing.

9. Opportunities for Future R&D and Testing Efforts

The most obvious opportunity for follow up is to test these techniques with better, more consistent input imagery and compare the results to an independent validation data set in order to correctly assess the accuracy. Based on its specification and past experience, the sensor holding most promises at this point in time is the Leica ADS40v2, which also happens to have been selected by Ontario to gather data for the next forest resource inventory cycle. Flight lines of the ADS40v2 over our test areas would be desirable, especially if the overlap can be such as to allow the software to concentrate on areas at $\pm 15^\circ$ from nadir.

Further work on determining the time savings of this semi-automated approach as compared to the conventional approach and, on quantifying the ‘tangible advantages’ of having a more objective process, should also contribute to advancing the concept of the ‘semi-automated individual tree crown’ inventory approach.

Apart from testing the *ITC Suite* on a better image data set, there are also opportunities in investigating the effects of different pre-processing steps to make the imagery more amenable to automated analysis techniques. The application of the BRDF correction to ‘rawer’ imagery, as opposed to the orthophotos already mosaicked, is thought to have much promise for improving the results. Investigation is needed into the number and nature of features that are needed for optimal BRDF corrections (i.e., a vegetation mask vs. separate softwood and hardwood masks).

Numerous software improvements are possible to the *ITC Suite*. For examples, as soon as PCI releases a ‘Lite’ version of their Software Development Kit, the Suite could be made compatible with PCI Geomatica v10 and above. On the other hand, it could be made completely independent of the PCI image analysis system using public domain software packages. The programs of the *ITC Suite* could also be organized to load partial images into memory rather than full images, especially if Microsoft is to be slow in releasing a decent and accepted 64-bit operating system.

On the research and development side, there is an obvious need to integrate automatic and/or semi-automatic ways to remove outliers from the signature generation process. Both ways should offer some ITC multispectral values plotting capabilities. Another

need, highlighted by the poor separability of the white pine species, is the need to introduce some crown structure elements to the classification process.

Research into optimizing the field data intensity and distribution of samples to support automated species identification at the same time as volume assessments is also needed. There is also a need to validate other key inventory attributes at the same time (stems per hectare, height, crown closure, etc.). Although the conventional way of calculating volumes is still possible and should produce better results when based on better species composition estimations, we need to demonstrate that volume estimations based on ITC crown area and their height, with mitigating factors such as stem density or site index, are indeed possible and, moreover, represent an improvement on the conventional approach. Given such demonstration, we need to later examine how improved crown delineation of both coniferous and deciduous tree could improve these calculations.

Bibliography

Castilla, G. (2006). Actualización semiautomática de la malla de recintos del Mapa Forestal de España. *Investigación Agraria. Sistemas y Recursos Forestales*. Fuera de serie: 14-23.

Cole, B. and Mallory, E. 2005. Swan Lake Forest Research Reserve – 20-year Management Plan: 2005:2025.

Gougeon, F.A. 1995. A crown-following approach to the automatic delineation of individual tree crowns in high spatial resolution aerial images, *Canadian Journal of Remote Sensing*, 21(3): 274–284.

Gougeon, F.A. 1997. Recognizing the forest from the trees: Individual tree crown delineation, classification and regrouping for inventory purposes, *Proceedings of the Third International Airborne Remote Sensing Conference and Exhibition*, Vol. II, Copenhagen, Denmark, 07–10 July, pp. 807–814.

Gougeon, F.; Cormier, R.; Labrecque, P.; Cole, B.; Pitt, D.; Leckie, D. 2003. Individual Tree Crown (ITC) Delineation on Ikonos and QuickBird Imagery: the Cockburn Island Study. In 25rd Canadian Symposium on Remote Sensing / 11e Congrès de l'Association québécoise de télédétection, Montréal (Québec), Canada, Oct. 14-17, 2003.

Gougeon, F.A.; Labrecque, P.; Guérin, M.; Leckie, D.G.; Dawson, A. 2001a. Détection du pin blanc dans l'Outaouais à partir d'images satellitaires à haute résolution IKONOS. *Dans Actes du 23e Symposium canadien de télédétection/ 10e Congrès de l'Association québécoise de télédétection (CDROM)*, Sainte-Foy (Québec), Canada, 21-24 août 2001. Institut aéronautique et spatial du Canada, Ottawa.

Gougeon, F.A.; Leckie, D.G.; Scott, I.; Paradine, D. 1999. Individual tree crown species recognition: the Nahmint study. Pages 209-223 *in* D.A. Hill and D.G. Leckie, eds. *International Forum - Automated Interpretation of High Spatial Resolution Digital Imagery for Forestry*. Victoria (Colombie-Britannique), Canada, 10-12 février 1998. Ressources naturelles Canada, Service canadien des forêts, Centre de foresterie du Pacifique, Victoria (C.-B.).

Gougeon, F.A.; Leckie, D.G. 2001. Individual tree crown image analysis: a step towards precision forestry. *In Proceedings of the First International Precision Forestry Symposium (CDROM)*. Seattle, Washington, USA, 17-20 juin 2001. University of Washington, Seattle.

Gougeon, F.A., and Leckie, D.G. 2003. Forest information extraction from high spatial resolution images using an individual tree crown approach, Natural Resources Canada,

Canadian Forest Service, Pacific Forestry Centre, Victoria, British Columbia, Information Report BC-X-396E, 27 p.

Gougeon, F.A. and Leckie, D.G. 2006. The individual tree crown approach applied to IKONOS images of a coniferous plantation area. *Photogrammetric Engineering and Remote Sensing*, 72(11):1287-1297.

Gougeon, F.A.; St-Onge, B.A.; Wulder, M.; Leckie, D.G. 2001b. Synergy of airborne laser altimetry and digital videography for individual tree crown delineation. *In Proc. 23rd Canadian Symposium on Remote Sensing/10e Congrès de l'Association québécoise de télédétection (CDROM)*, Sainte-Foy (Québec), Canada, 21-24 août 2001. Institut aéronautique et spatial du Canada, Ottawa.

Leckie, D.G.; Gillis, M.D. 1995. Forest inventory in Canada with emphasis on map production. *Forestry Chronicle* 71(1): 74-88.

Leckie, D.G.; Gougeon, F.A. 1999. An assessment of both visual and automated tree counting and species identification with high spatial resolution multispectral imagery. Pages 141-152 *in* D.A. Hill and D.G. Leckie, eds. *International Forum - Automated Interpretation of High Spatial Resolution Digital Imagery for Forestry*. Victoria (Colombie-Britannique), Canada, 10-12 février 1998. Ressources naturelles Canada, Service canadien des forêts, Centre de foresterie du Pacifique, Victoria (C.-B.).

Leckie, D.G. Gougeon, F.A. Hill, D.A. Quinn, R. Armstrong, L. and R. Shreenan 2003. Combined high-density LiDAR and multispectral imagery for individual tree crown analysis. *Canadian Journal of Remote Sensing* 29(5): 633-649.

Yuan X et D.G. Leckie, 1992. An investigation of correction techniques for view-angle effects on high-resolution MEIS data of forested terrain. Dans : 15^{ème} Symposium Canadien de Télédétection. Toronto, Ontario, Canada. 462-467.

Appendix 1

The Semi-Automatic Individual Tree Crown Approach to Forest Inventories: Special Considerations with Aerial Images

Introduction

Although developed initially using aerial sensor multispectral images with a spatial resolution of around 60 cm/pixel, the Individual Tree Crown (ITC) approach (Gougeon & Leckie, 2003) mostly made its mark in the present decade due to the availability of high resolution satellites, such as IKONOS and QuickBird. These two satellites offer panchromatic spatial resolutions of the order of 1 m/pixel and 61 cm/pixel, respectively, with cruder multispectral resolutions of 4 m/pixel and 2.44 m/pixel, respectively. Their spatial coverage of 11x11 km² and 16.5x16.5 km² makes them particularly attractive, as the analysis a single image produces results that often encompass the coverage of a typical forest inventory map sheet. Before this decade is over, numerous other high spatial resolution satellites are due to join them in orbit, increasing sharply the availability of this type of data.

Although such spatial resolutions allow for most dominant and co-dominant individual tree crowns to be seen, separated, and classified into species, successful results have been achieved (and verified) mostly at the stand composition level, after the individuals were regrouped. By itself, the added precision on stand species composition should have drastic effects on volume assessments and provincial estimations of allowable cut, even when using the conventional approach in their estimation (i.e., regrouping stands into strata to which volume assessments from plot measurements are connected). However, this has not been formally demonstrated at this point in time. Nevertheless, it is an inference that we are willing to make knowing that on average, interpreters are only 50-65% accurate on the main (or sole) species in stands, and that this accuracy drops drastically in mixed stands (Quebec - Rapport Coulombe, p. 166; Ontario - Forestry Chronicle, March 2007; British Columbia - Web Site on TFL/TSA inv. Audits)

Unfortunately, for numerous reasons (clouds, haze, large view angles, priority USA contracts, wrong seasons, etc.), the availability of good quality high resolution satellite images is still poor. This problem should alleviate itself fairly soon as numerous other satellites of this calibre are expected in the coming years due to high demand and private sector sponsorships. In addition, some of these satellites will fly under the same banner, such that a single order could possibly apply to more than one satellite. Also, image data will have accumulated in databases (private and governmental), making it easier to find proper images from the proper time period (i.e., in most places, for forestry, about 6–8 weeks around July), especially considering that forest inventory cycles typically span many years (7–10 years for most provinces).

Similarly, the availability of digital aerial images is sharply on the rise as numerous good quality sensors exist and because imagery is often acquired to systematically populate databases from which it is later purchased (NorthWest Geomatics, ADS40 acquisitions). In addition, the forest inventory community (i.e., the provincial governments, the forest companies) is moving to a soft-copy interpretation approach, discovering the added benefits of direct GIS compatibility and the pleasure of multispectral image interpretation; while retaining one of the main benefit from the past, that of controlled acquisition conditions via specific contracts. However, the use of the semi-automatic ITC approach to forest inventories on large areas covered by aerial images (or strips) has not been fully demonstrated yet.

The process to achieve an ITC-based forest inventory for a given region using aerial images is essentially the same as the one outlined for satellite images in the BCX-396 report (Gougeon & Leckie, 2003). However, because there are substantial differences between the two types of images, due to the sensors themselves or to the way the images are acquired and pre-processed, the ITC analysis process entails numerous additional considerations to insure good species recognition. These considerations are discussed in the following section following a brief introduction to sensor technology.

Aerial Sensor Technology

In the field of digital remote sensing (DRS), there are three types of well know multispectral satellite sensors. First, sensors such as the one found on the Landsat satellite series that gather data one pixel at the time while using an oscillating mirror that sweeps across the field of view to create the image lines. Second, the so-called 'push-broom' sensors *à la* SPOT, that gather one image line at the time with a linear array (i.e., a line) of Charge-coupled device (CCD) photosites. Third, the 'full frame' sensors like IKONOS or QuickBird that gather a full two-dimensional (2D) scene with one 2D CCD sensor per spectral band. All of these use prism or gate diffraction to gather the data in the other spectral bands.

A common feature of satellite images is their acquisition from a high altitude (600-800 km) allowing them to cover substantial areas of the ground while using lenses exhibiting very small view angles (2–3°). Compare to aerial images, this simplifies substantially the pre-processing needed before an ITC analysis can be carried out, as objects (trees) are essentially all seen from above (i.e., no leaning to the side) and most importantly, are all part of the same scene. However, it should be noted that some satellite sensors can be rotated to look to the side, thus increasing the probability of an acquisition, but creating images where objects are seen with significant view angles.

The satellite sensors described above all sprung from developments made first on aerial sensors. This trend continues, albeit mostly outside of Canada now. For examples, the Deadulus series of airborne sensors sponsored a Landsat-type sensor, while the MEIS, the Casi, the DMZ, or the Leica sensors, to name but a few, followed a push-broom

approach. In addition to using multiple linear arrays to gather the multispectral data at nadir, many of these sensors also have similar acquisition capabilities looking forward and looking backward, thus creating multispectral stereo pairs for the more ‘traditional’ interpretive approaches (now done on computers, in the so-called soft-copy environment). The Casi is essentially a hyperspectral sensors that can be used in multispectral mode, but typically producing more spectral bands than the ubiquitous four (nIR, R, G, and B). Sensors like that of Kodak or Applanix use the 2D frame camera approach, with or without stereo pair capabilities. Others sensors are even more sophisticated. Example systems and types are presented in Table A1–1.

Table A1–1. Types of airborne and satellite sensors.

| Type of sensors | Examples |
|--|---------------------------------|
| Mechanical scanner (oscillating mirror, one pixel) | Landsat, Deadalus |
| Push broom sensors (one line at the time) | MEIS, Casi, ADS40(v1,v2) , SPOT |
| Frame cameras (2 dimensions) | Kodak, DMC, Applanix, ALTM |
| Frame camera with pan-sharpening | IKONOS, QuickBird, ... |
| Wide push broom sensors (more than one line) | M7VI (v1, v2, v3) sensors |
| Others (time synchronization and pan-sharpening) | Vexcel UltraCam |

The Vexcel UltraCam system uses a sophisticated system of gathering panchromatic image parts through time, while getting its multi spectral channels from single 2D arrays. It thus has to reconstruct the panchromatic image from all these frames, relying on correlation within overlapping image regions to make a single grey-level high definition scene, and on pan-sharpening techniques to produce a multispectral high definition image. Note: multiple lenses are involved. Making corrections (such as those for vignetting) are more complicated. Sections of what would be considered a single image can be off in relation to others.

On the other hand, the M7VI sensor uses an approach that sits in between the 2D frame camera capturing a full scene and the linear arrays capturing a single line of image at a time. It could be considered a wide push-broom approach, gathering data a few hundred lines at a time, yet delivering data in long strips like that of a push-broom sensor. In addition, up to five cameras (thus five lenses) are used in parallel to create a wider strip, leading to numerous artefacts in both image strip directions.

As a final note here: a warning that pan-sharpening, whether with satellite or airborne sensors, done on-the-fly on board the sensor or on the ground after the acquisition is done can often be misleading. It is important to always keep in mind that the multispectral data was acquired at a cruder resolution than it appears (often by a factor of four) and that this will affect (to a certain extent) the delineation of tree crowns, but more importantly, their species recognition. Indeed, most multispectral pixels that appear to be well within a tree crown will have had their value affected by what is around that tree crown, be it shade, another crown, or background vegetation or material.

Image needs for computer image analysis

One common mistake is to make the assumption that because imagery is acquired by a digital sensor it is automatically suitable for the production of forest inventories via semi-automated computer image analysis approaches. It is important to point out that the image requirements of computer image analysis can be quite different from that of soft-copy interpretation. Obviously, this must be taken into account when specifying the deliverables for an aerial acquisition mission, as the typical products will have been designed for the interpretation realm. The differences are significant on many levels (see Table A1–2). At a first obvious level, soft copy interpretation typically requires stereo pairs with a good base line and sizeable image overlaps, while orthophotos or long georeferenced image strips are generally preferred for computer image analysis. Generally, the soft copy image interpretation realm favours good image and cursor handling capabilities, faster image loading and roaming speed, and a facility of movement from one stereo pair to another without losing context and position; while computer image analysis needs *sine qua none* to be able to insure radiometric consistency throughout the area to be analysed.

Table A1–2. Typical image needs for soft copy interpretation and for computer image analysis.

| Soft-Copy Interpretation | Computer Image Analysis |
|--|--|
| Colour-balanced stereo pairs (with a good base) with a colour-balanced orthophoto mosaic as reference | Separate sizeable orthophotos or long georeferenced image strips (no artificial stretches or colour balancing) |
| Pan-sharpened (RGB,CIR, RGBI) are preferred | Can benefit from separate panchromatic and prefers as many bands as possible |
| 8 bit images are sufficient and preferred | Images reflecting the capabilities of the sensor (8, 12, 14, or 16 bits of radiometry, in 8 or 16 bit image files) |
| Images are preferred compressed, with a pyramid of resolutions for faster loading and fast scale changes | Only lossless compression tolerated. Some additional pyramids for visualization as a convenience |
| Sizeable ground area covered (for context) with large image overlap for stereo viewing | Long strips will improve BRDF corrections and make ITC analysis more efficient (with overlap to concentrate on $\pm 15^\circ$ off-nadir) |

With careful planning and good discussions with the aerial data providers, it is possible from a single mission to order data in all of the formats necessary for both soft-copy interpretation and computer image analysis, at very little incremental cost.

BRDF correction and normalization across the whole dataset

Ensuring radiometric consistency throughout the forested area to be analysed is essential for species recognition via digital image analysis. Methods on “How can this be achieved?” and “Why is it desperately required?” are presented below. The last question is the easiest to answer and will be addressed first.

Most of the processing tasks in the computer image analysis (i.e., ITC analysis) of a given forested area covered by satellite or aerial images can be made fairly automatic. The most significant human contribution, apart from specifying acquisition requirements and organizing the datasets, is in the training of the ITC classifier to recognize the forest species of interest. It consists mostly in identifying to the computer software sample trees, or preferably single species sample areas (fastest), representative of all the species of interest, and sometimes, even of species in a specific situation (e.g., trees of species A on sun facing slopes, trees of species A on North facing slopes, mature trees of species A, juvenile trees of species A). Good interpretive skills and auxiliary data are needed for this endeavour. Knowing which situations to depict to the computer can be an art as well as a science. Of course, the purpose is to create spectral, textural, structural, and contextual signatures that are representative of the species in given situations, in order for these signatures to be used to classify the bulk of the trees in the images. If these samples are to be picked up anywhere in the images or, from any of the images, and if the resulting signatures are to be applied to the full forested area to be analysed, all of these images will need to be radiometrically corrected and normalized to each other.

How do we achieve this? What are the factors affecting the uniformity of radiometry throughout a series of aerial images? What are the factors on a single aerial image?

The first and most important factor affecting the radiometry on a single aerial image is certainly vignetting. By vignetting we mean, the radial variations in apparent colour from the centre to the boundaries of the images due to the optic properties of the lenses and due to objects increasingly appearing to lean from the nadir view (above view) at the centre of the aerial image. This is caused by the use of a wide angle lens (50-65° vs. 2-3° for satellite sensors) needed to cover large areas at low altitude. The second most important factor is the sun’s illumination angle making the objects on one side of the image essentially backlit, while they are front lit on the other side.

Differences in radiometry between aerial images are often attributable to the use of automatic exposure calibration (i.e., variable aperture and/or shutter speed), different acquisition times and atmospheric conditions (as neighbouring lines are rarely sequential in time), the presence of clouds and/or cloud shadows, and often, as orthophotos are generally preferred by groups without stereo viewing capabilities, the normalization and calibration processing, and the manual interventions (e.g., cloud removal) that are typically involved in making such mosaics as seamless as possible.

Push-broom sensors, gathering aerial images one line at the time, do not exhibit the radial distortions found with frame (2D) cameras, but they are affected by the sun’s illumination

angle and their wide across track view angle. Both these affects can be parameterized and partially alleviated by what are known as BRDF corrections. Such corrections attempts too make the radiances on both sides of an image similar to that at the image centre (i.e., at nadir). For a given sun illumination angle (azimuth and elevation), the bi-directional reflectance distribution function (BRDF) fits a curve to the distribution of radiances from one side of the image to the other. The correction aspect consists in subtracting the inverse of the curve from the data, after having normalized it to have zero difference at nadir. In addition, by imposing a specific value (i.e., one for each band) at nadir to all the images, one can further **normalize images between one another**.

Although a normalization between images can be achieved with some sort of histogram equalization (or histogram matching), such process are typically adversely affected by the quantity of non-vegetation material (such as lakes, swamps, dead trees, sandy and rocky areas) present in a given image. Similarly, with BRDF corrections, vegetation is best corrected by analysing data gathered only from the vegetation. Such data should preferably be gathered from long strips to minimize the effects of species composition within the forested areas. To be more precise, data can also be gathered from numerous features (e.g., water, softwood, hardwood) such that multiple correction curves are applied to the image, one for each such feature. The small, conically-shaped coniferous trees will typically have a different BRDF than the bigger, more rounded crowns typical of hardwood trees. Ideally, a weighted correction curve taking all features simultaneously into consideration should be applied (Yuan and Leckie, 1992) to avoid possible discontinuities.

The radial distortion patterns found with frame cameras can also be partially alleviated using a proper radial correction function or at least, by running BRDF corrections in both directions, which is what was done in this project for the Vexcel UltraCam images.

BRDF corrections as used in this project

Given the above, a fair question to ask is: Why did BRDF correction fail us in this project? There are multiple reasons, some of which are different depending on which of the two sensors was involved. We will elaborate further below. However, the main reason is that BRDF corrections, with their potential for image to image normalization, **should be applied before most image manipulation and pre-processing**.

Over time, in order to facilitate production runs, the *ITC Suite* BRDF correction program has been modified to deal with situations that are increasingly different from ideal situations of working on raw, or almost raw images. For example, in a raw image or a raw image strip, the location of nadir (essential for proper BRDF corrections and normalizations) is at the centre of the image and typically, at the centre of the image file. As soon as such an image (or strip) is georeferenced, although nadir is of course still at the centre of the image, it is unlikely to be at the centre of the image file (unless the flight line was perfectly aligned North). The developed BRDF program has options to deal with such situations. Similarly, when the acquisitions from many flight lines are put together

in a single georeferenced file, the program was modified to deal with multiple flight lines (i.e., multiple nadir, multiple correction curves). However, the assumption was that whoever did the mosaicking of these flight lines would tend to keep the centre of each line (i.e., the data least affected by the wide view angle) and that the seam lines on both sides of each strips would be kept rather straight (as in Figure A1-1))

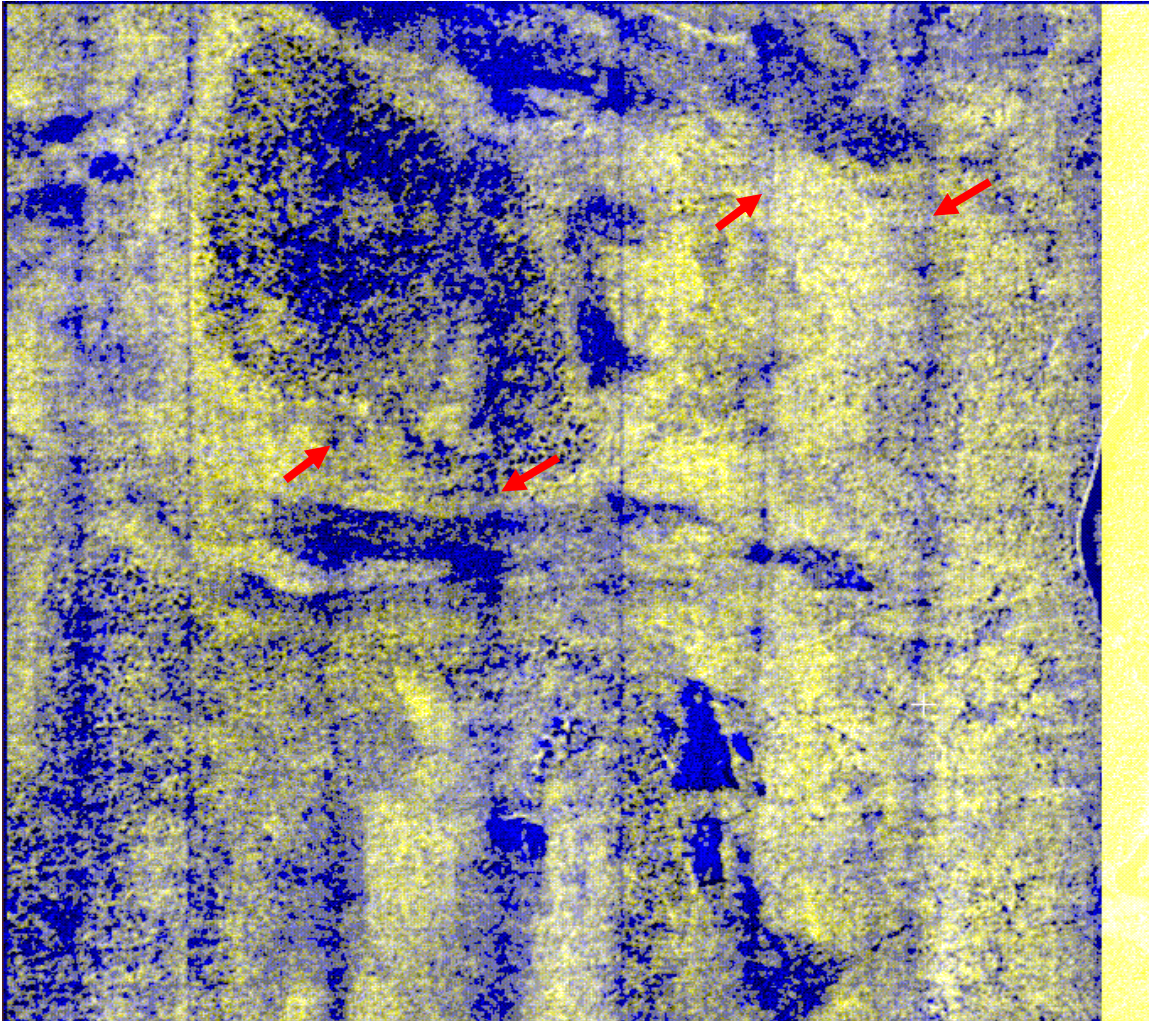


Figure A1-1. Colourful rendition of a texture analysis of a M7VI image tile where three distinct mosaicked image strips are visible. Here, the problem is compounded by the fact that each image strip is also acquired with three distinct lenses (blurrier vertical lines pointed to by red arrows).

The *ITC Suite* BRDF program was thus designed to deal with the situation depicted in Figure A1-1. Image strips collected with the use of multiple lenses could be dealt with by treating them as distinct flight lines. However, in the case of the M7VI data, the wide push-broom approach mentioned above prevented us from getting good radiometric

consistency. It was not possible to correct for the vertical aspect of the radial distortion, as image tiles from 100–300 lines are arbitrarily picked up in the vertical direction (see effects depicted in Figure A1–2).

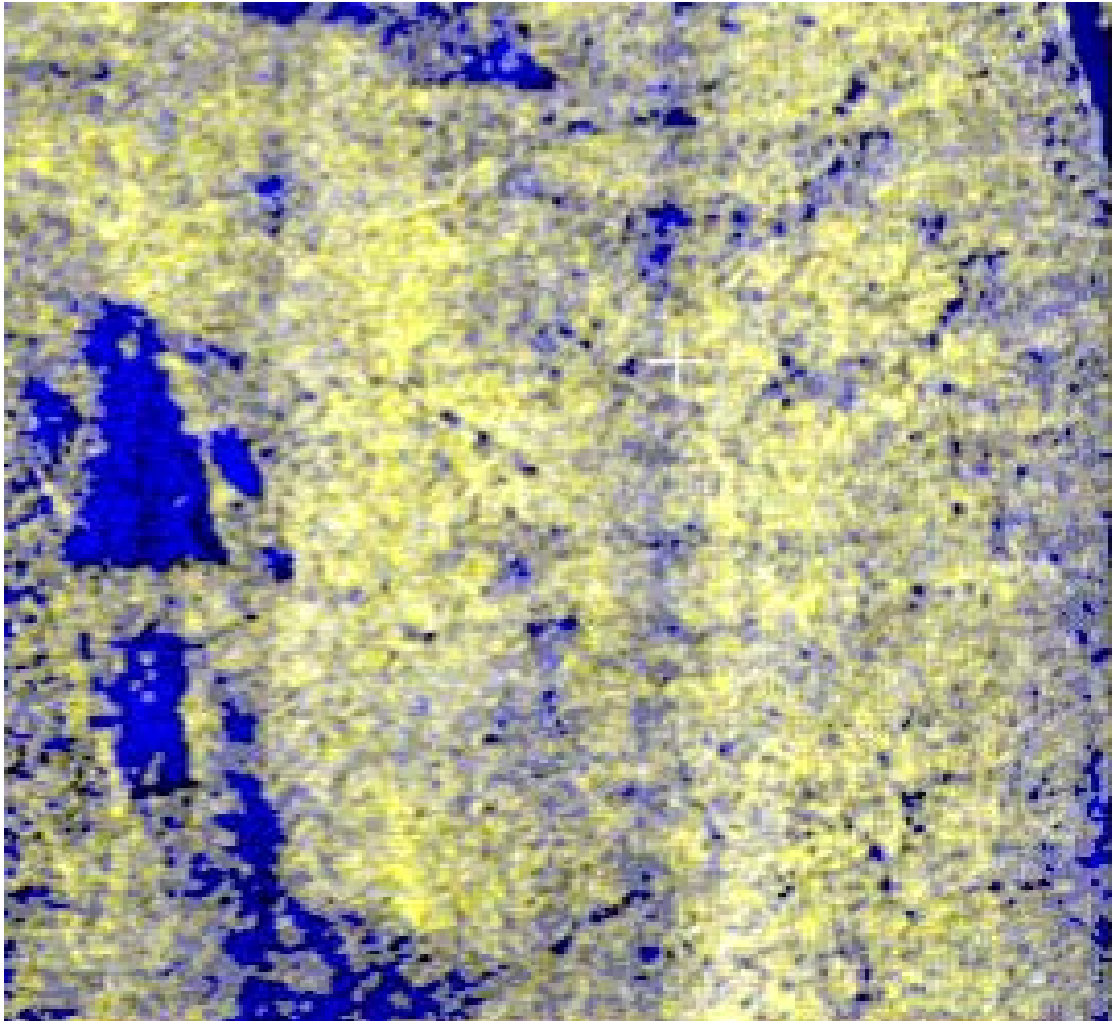


Figure A1–2. Colourful rendition of a texture analysis of a M7VI image tile showing the ripples caused by the vertical aspect of the radial distortion, as image segments made of 100–300 lines are arbitrarily picked up in the vertical direction to create the image.

In the case of the Vexcel Ultracam data, the OrthoEngine software from PCI had been used to create the mosaic from the raw images. It makes automatic decisions about colour balancing and where to create seams. As can be seen in Figure A1–3, it seems strongly biased towards keeping image sides rather than image centres. In this case, because the flight lines were west to east, it seems biased toward keeping the bottom half of the original images.

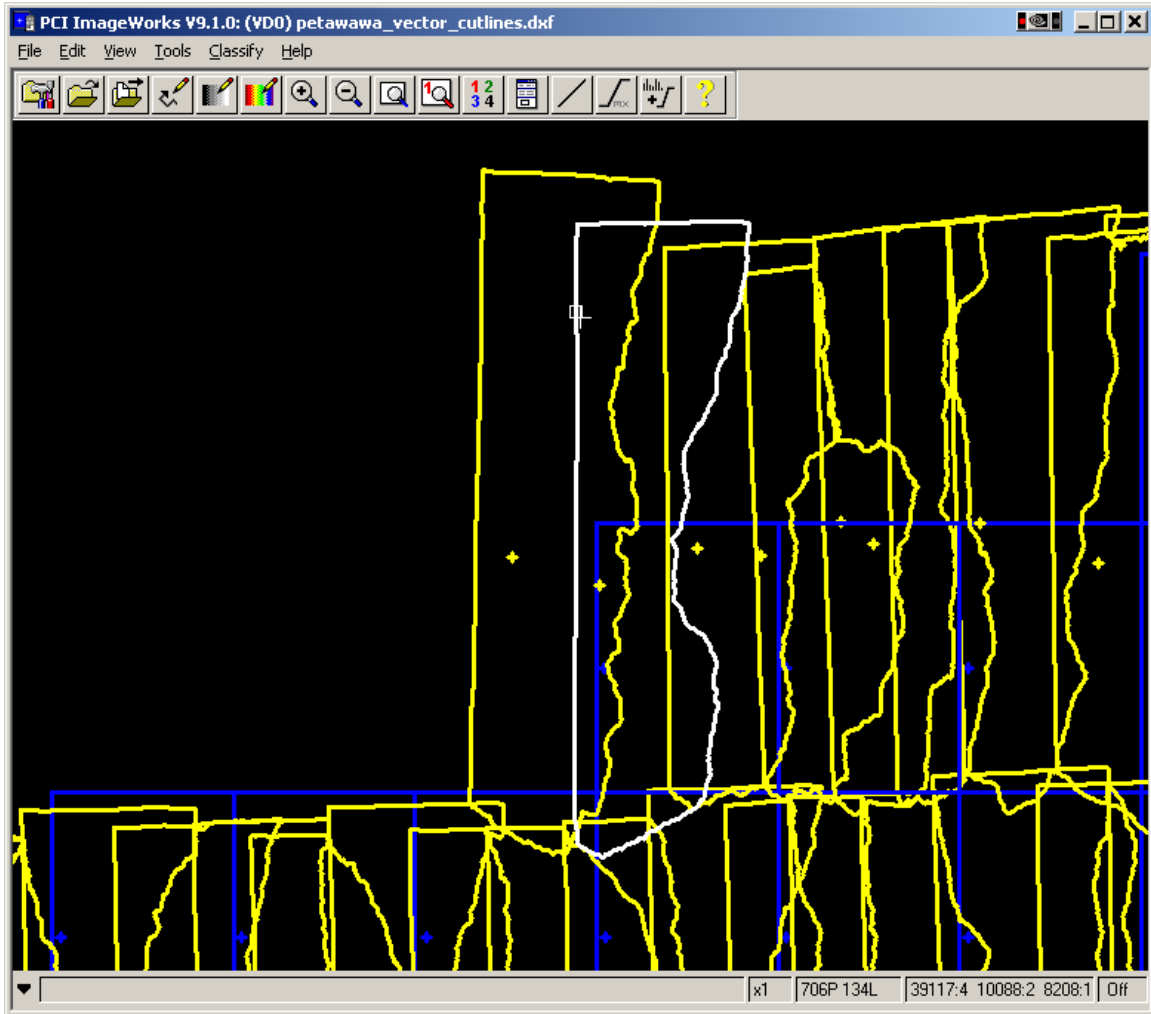


Figure A1-3. Seams line automatically generated by PCI™ Orthoengine used to create the Vexcel orthophoto mosaic. Tiles (individual files) of the mosaic are shown in blue, while segment of original Vexcel images are shown in yellow, with one highlighted in white. The images were acquired during West to East flights.

The effects on a single 1 km by 1 km tile can be seen in Figure A1-4. These problems are compounded by the fact that manual editing (cut and paste) took place to remove clouds and cloud shadows, as seen by the two obvious ‘thumbprints’ at the bottom left of the image in Figure A1-4.

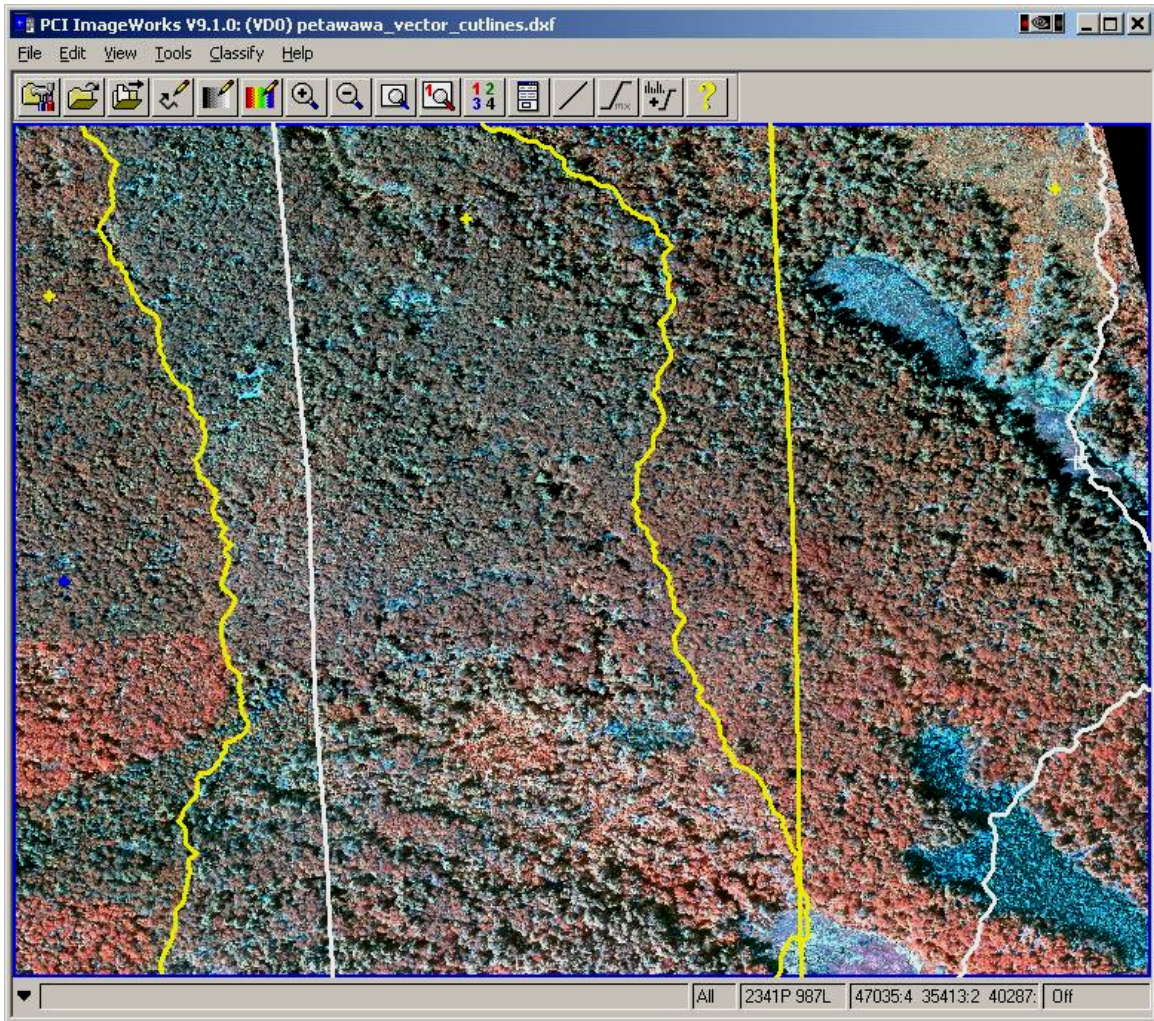


Figure A1–4. Example of the different image sections that can be found within a 1 km² tile of the Orthophoto of Vexcel images. A serious overkill considering the original images covered at least 2 x 3 km². Just picking up the centre 1 km² would have been a far superior approach. Also visible on the bottom-left are the effects of cloud removal by manual editing (no information existed as to the provenance of such image sections).

The whole process of mosaicking and of hiding seam lines with smoothing create numerous artifacts, although some of the blurriness of sections of images must be due to the acquisition process (as seen in Figure A1–5).

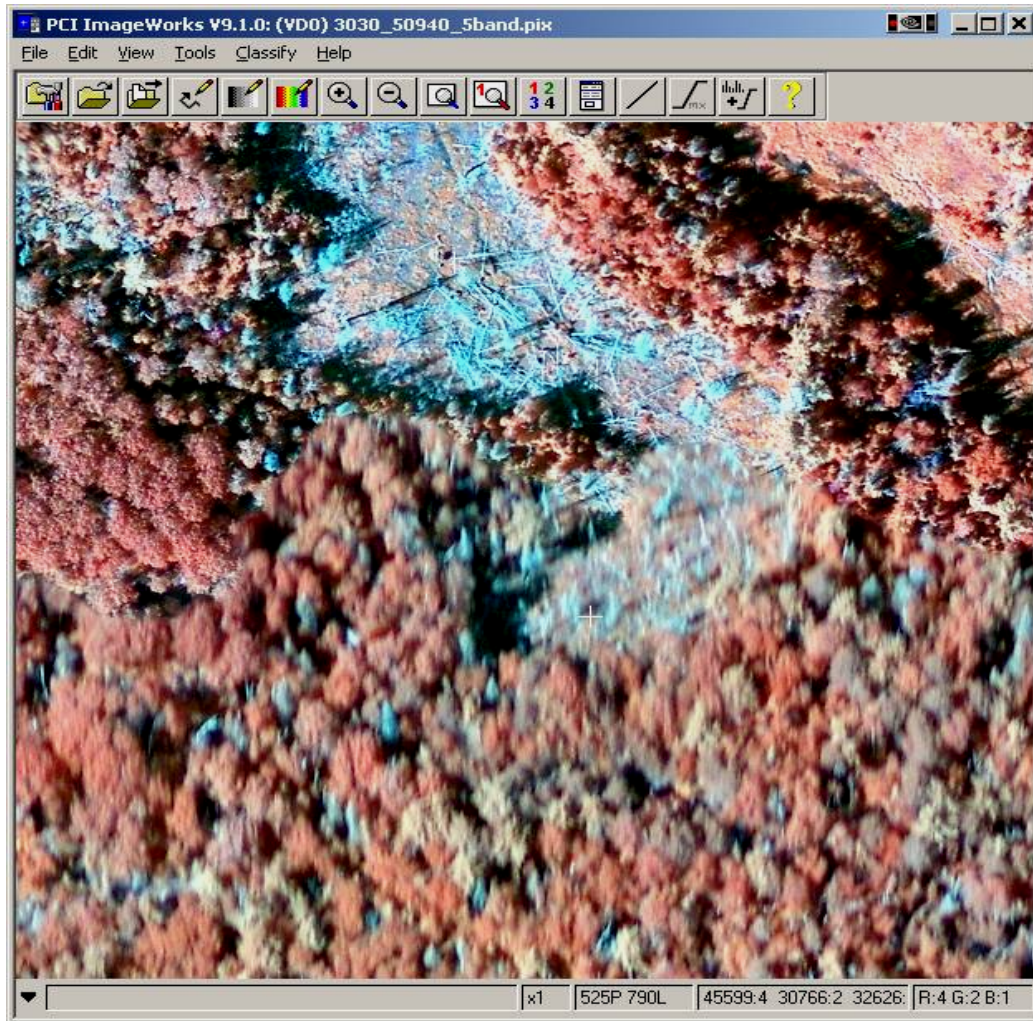


Figure A1–5. The blurriness of the bottom part of the image can not be explained by just an attempt to blur the image around the mosaic seams.

Independent of the issues just outlined relative to not being able to perform good BRDF corrections and normalization on the Vexcel UltraCam data (as with the M7VI data) is the intrinsic (on board?) pan sharpening based on a fragmented panchromatic image. Recall from the specifications of the Vexcel Ultracam sensor that it gathers its panchromatic image from 9 segments, using 4 different lenses (as shown in Figure A1–6). This appears to sometimes lead to sections of images not having the same radiometric balance than others, as shown in Figure A1–7.

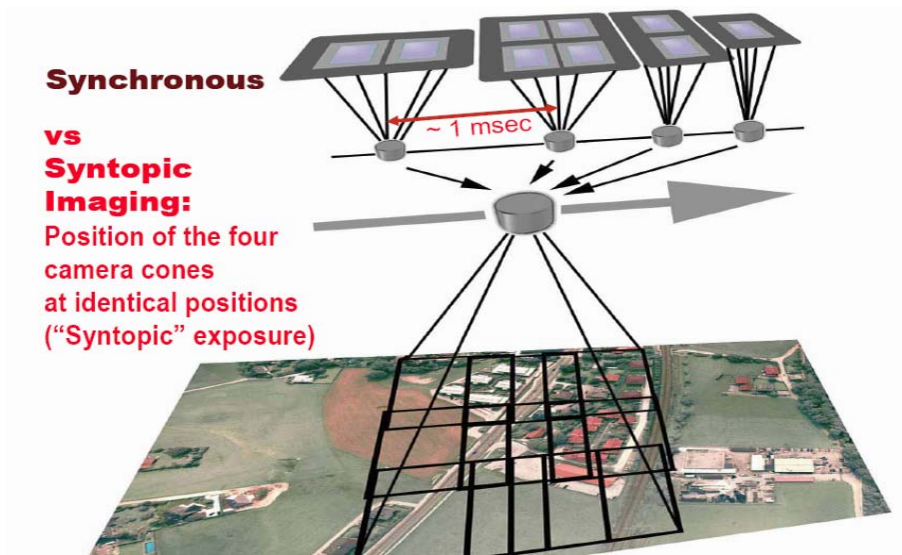


Figure A1-6. How the Vexcel panchromatic images are acquired.

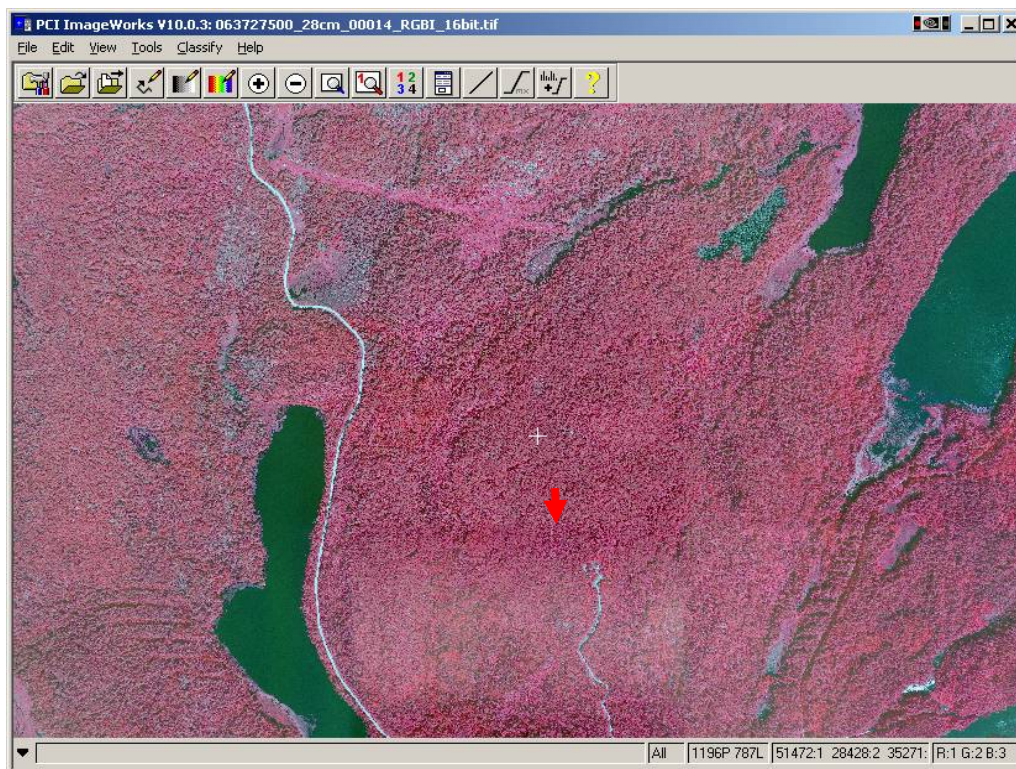


Figure A1-7. The bottom centre portion of this image appears covered with haze, but this is actually due to improper adjustment between the 9 different panchromatic sections of the image.

Presumably, lots of the sensor and pre-processing issues mentioned so far (and there are numerous others) could be alleviated, if not completely removed, by good and honest discussions with the data providers, assuming they have knowledgeable staff on hand, are willing to discuss the issues, and care about clients wanting to do digital analysis of their images.

From past experiences with line imagers, from its specifications and from preliminary analyses of some of its images, the Leica ADS40v2 sensor, recently selected by Ontario for its next forest inventory round, appears to be a much more appropriate sensor, provided that one can get access to the raw flight lines and that flight lines overlap is sufficient to minimize angle of lean ($\pm 15^\circ$ off-nadir).

Tests of feature-based BRDF correction curves on two ADS40-v2 flight lines.

Two neighbouring flight lines from a Leica ADS40-v2 sensor were selected to test a variety of BRDF corrections. Two test areas, one of softwoods and one of hardwoods, were created in the overlapping region of two flight lines (see Figure A1–8). The differences in radiances of the ITCs within these two test areas on each image are going to be monitored for BRDF correction curves generated from a variety of increasingly precise features.

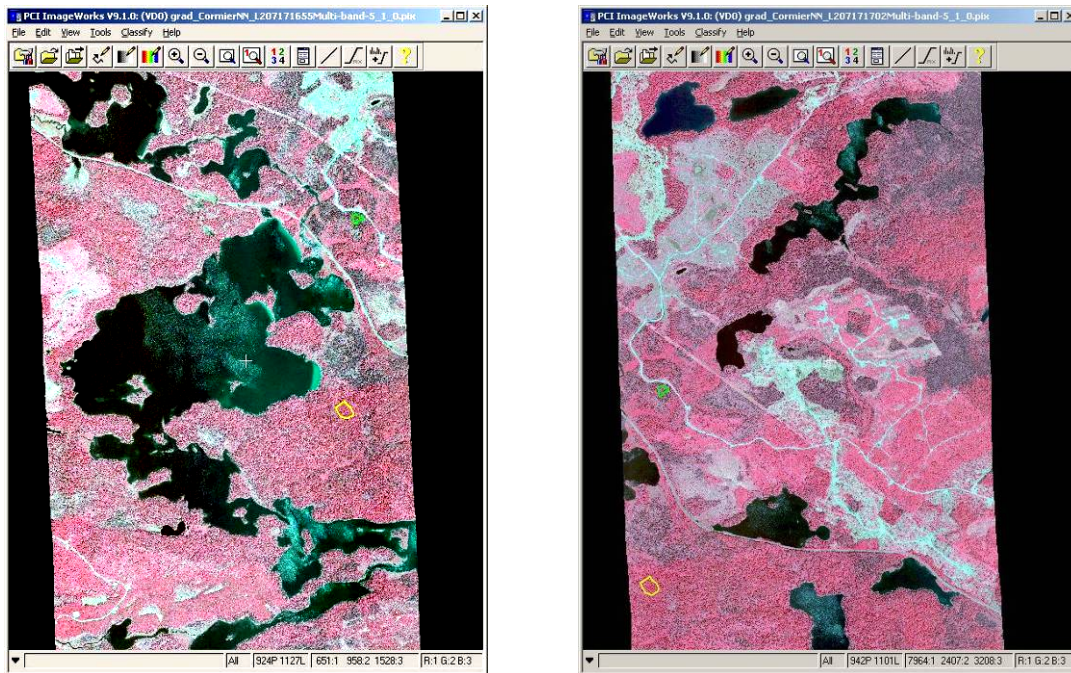


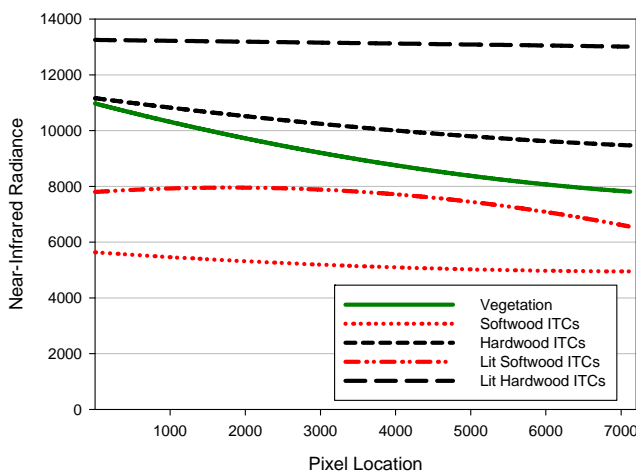
Figure A1–8. Two test areas, one of softwoods and one of hardwoods, were created in the overlapping region of two flight lines from a Leica ADS-40v2 sensor to test the correction capabilities of various BRDF curves (courtesy of Bowater and R&B Cormier).

Traditionally, BRDF correction curves are generated by accumulating the radiance values within each image column (i.e., at each pixel position), for each spectral band. The effects are generally more pronounced with the near infra-red channel. For a given spectral band, such histogram displays the illumination trends as one gets away from nadir. A curve is fitted to the histogram and the radiance at nadir is subtracted from the curve to make it relative to nadir. The inverse of the curve is applied to the image data, on a line-by-line basis, to correct its radiances for the BRDF effects.

Unfortunately, this classic approach is strongly influenced by the image content. For example, the presence of more lakes or more cut over areas on one side of the image will strongly (and adversely) influence the correction curve. A first order improvement to this approach, consist in first creating a mask of vegetative areas and then, only collecting data underneath that mask.

A potential improvement, one easily achieved in our context, is to use the ITC mask rather than a vegetation mask. This allows the correction curve to concentrate on the effect of BRDF on trees, which may be different than that on other low lying vegetation. As trees react differently to the combination of illumination and view angles due to their different shapes and branching patterns, a further improvement could potentially be achieved by using different masks (thus, correction curves) for hardwood and softwood trees. In addition, since the individual tree crowns generated by our crown delineation process contain the shade side of each tree, another improvement could potentially be achieved by only picking-up the lit-side of each crown. After all, the lit-side of each tree crown is what will be used in the ITC classification process, thus, better to optimize the correction of radiances within that context. Such feature-specific BRDF curves are shown in Figure A1–9.

Near-Infrared Radiance for Hardwood and Softwood ITC Conditions



From the curves in Figure A1–9, one can see that trees (and vegetation in general) are much brighter on the left side of the image, and that hardwoods are less affected by the phenomenon than softwood, towards the extreme case, where the lit-side of hardwood tree crowns appear barely affected at all. The results of the various feature-based correction curves are shown in Table A1–3.

Figure A1–9. Curves (for the near infrared band) of radiance tendencies due to the joint effects of the solar illumination angle and the view angle gathered under increasingly specific feature mask (from the left side image in Figure A1-8)

Table A1–3. Differences in radiances between tree crowns from two test areas softwoods, hardwoods) from the overlapping zone of two flight lines after different types of feature-based corrections for view and illumination angles (BRDF corrections).

| Feature-based BRDF correction types | | | | | | | |
|--|----------------------|---------------------|-------------------------|------------------|-----------------------|------------------|-----------------------|
| Cover type | Spectral band | Without BRDF | Vegetation based | ITC based | ITC(lit) based | ITC (S/H) | ITC(lit) (S/H) |
| Softwood | nIR | 24% | 2.1% | 1.1% | 0.5% | 2.6% | 6.9% |
| | Red | 31% | 9.3% | 4.6% | 10.6% | 5.7% | 1.3% |
| | Green | 29% | 7.2% | 1.6% | 7.5% | 5.8% | 1.4% |
| Mean | | 28% | 6.2% | 2.4% | 6.2% | 4.7% | 3.2% |
| Hardwood | nIR | 14% | 3.9% | 4.6% | 5.7% | 2.4% | 5.5% |
| | Red | 6% | 22.7% | 22.3% | 16.6% | 10.8% | 2% |
| | Green | 14% | 9.2% | 9.5% | 6.5% | 7% | 3.3% |
| Mean | | 11% | 11.9% | 12.1% | 9.6% | 6.7% | 3.6% |
| In general | Average | 20% | 8.7% | 7.3% | 7.9% | 5.7% | 3.4% |

Table A1–3 displays a progression towards increasingly similar spectral signatures (for both softwoods and hardwoods) as the two overlapping images are corrected and normalized with BRDF correction curves based on increasingly precise features. As expected, the correction effects are more drastic on the softwood crowns, going from a difference between images of 28% without any correction, to only 3.2% with the best correction.

Conclusion

As discussed, not all data gathered by digital airborne sensors can be used fruitfully in computerized image analysis, even less when trying to achieve species recognition at the individual tree level. However in many cases, numerous difficulties can be alleviated by good *a priori* discussions with a knowledgeable data supplier. The acquisition should be planned with the computerized image analysis in mind. Data acquired for on-screen image interpretation may not be suitable for digital analysis, although the incremental cost of getting the data in two formats may be marginal.

Feature-based BRDF corrections, with their potential for intra- and inter-image normalization, are absolutely necessary to achieve good individual tree classifications of forested areas spanned by several flight lines. However, this is not a panacea. If residual differences of the order of 3.4% persist, there will still be more or less obvious classification errors, as species signatures are typically very close in spectral space. Whether these errors will still be of significance when the information is reported at the stand level will depend a lot on specific circumstances.

For this reason (and others, related to crown delineation considerations), we would recommend that flight line overlap by 15°, such that the ITC analysis can be concentrated on view angles that are $\pm 15^\circ$ off-nadir. Under such circumstances, the residual errors would probably be less than those reported above, as the testing areas here were situated at 20 and 25° off-nadir.